

113-th European Study Group with Industry (ESGI^o 113)

September 14-18, 2015
Sofia, Bulgaria

PROBLEMS & FINAL REPORTS



FASTUMPRINT
2015

Organizers:

Institute of Information and Communication Technologies, BAS,

**Faculty of Mathematics and Informatics,
Sofia University “St. Kl. Ohridski” and**

Institute of Mathematics and Informatics, BAS

in cooperation with

European Consortium for Mathematics in Industry

Scientific Advisory Committee:

Prof. Dr.Sc. Svetozar Margenov, Director of IICT, BAS

Doc. Dr. Evgenia Velikova, Dean of FMI, SU

Prof. Dr.Sc. Julian Revalski, Director of IMI, BAS

Local Organizing Committee:

Doc. Dr. Ivan Georgiev, IICT and IMI, BAS

Doc. Dr. Nadya Zlateva, FMI, SU

Doc. Dr. Krasimir Georgiev, IIKT, BAS

Doc. Dr. Neli Dimitrova, IMI, BAS

Prof. Dr.Sc. Stefka Dimova, FMI, SU

Doc. Dr. Todor Gurov, IICT, BAS

Doc. Dr. Nikola Naydenov, FMI, SU

Doc. Dr. Hristo Kostadinov, IMI, BAS

Dr. Stanislav Harizanov, IICT, BAS

Kristina Kapanova, IICT, BAS

Assoc. Prof. Tihomir Ivanov, FMI, SU and IMI, BAS

Dragomir Aleksov, FMI, SU

Galina Lyutskanova, FMI, SU

© Institute of Information and Communication Technologies, BAS, 2015

© Sofia University “St. Kl. Ohridski”, 2015

© Institute of Mathematics and Informatics, BAS, 2015

Published by FASTUMPRINT, Sofia, Bulgaria

ISBN 978-619-72-23-12-5

Contents

Preface	5
List of participants	7

Problems

Problem 1. <i>Chaos Group Ltd.</i> – Problem 1. Spline intersection improvement	11
Problem 2. <i>GemSeek</i> – Development of Mathematical Algorithm for Direct Ascription of Missing Values in Survey Research Data	13
Problem 3. <i>STOBET Ltd.</i> – Optimal Cutting Problem	15
Problem 4. <i>EngView Systems Sofia (A Sirma Group Company)</i> – The 2D/3D Best-Fit Problem	17
Problem 5. GEO RUHR , <i>Germany</i> – Analytical solution for consolidation of a soil layer with finite thickness under cyclic mechanical loading	21
Problem 6. <i>STEMO Ltd.</i> – Cyber Intelligence Decision Support in the Era of Big Data	24

Final reports

<i>D. Aleksov, M. Paskova, N. Naidenov, P. Marinov.</i> Spline Intersection Improvement	29
<i>V. Kolev, V. Noncheva, V. Valkov, E. Ilieva, M. Dobрева.</i> Direct Ascription of Missing Categorical Values in Survey Research Data	40

<i>A. Avdzhieva, T. Balabanov, G. Evtimov, D. Kirova, H. Kostadinov, Ts. Tsachev, S. Zhelezova, N. Zlateva.</i> Optimal Cutting Problem	49
<i>V. Bodurov, D. Dimov, G. Evtimov, I. Georgiev, S. Harizanov, G. Nikolov, V. Pirinski.</i> The 2D/3D Best-Fit Problem	62
<i>P. Iliev, S. Stoykov, B. Marković, M. Datcheva, L. Youkov, K. Liolios, C. Menseidov, N. Müthing, T. Barciaga.</i> Rigorous and Approximated Solutions of the Consolidation Problem for a Soil Layer with Finite Thickness under Cyclic Mechanical Loading	74
<i>Z. Minchev, G. Dukov, T. Ivanova, K. Mihaylov, D. Boyadzhiev, P. Mateev, M. Bojkova, N. Daskalova.</i> Cyber Intelligence Decision Support in the Era of Big Data	85

Preface

The 113th European Study Group with Industry (ESGI'113) was held in Sofia, Bulgaria, September 14–18, 2015. It was organized by the Institute of Information and Communication Technologies, Bulgarian Academy of Sciences (IICT-BAS), the Faculty of Mathematics and Informatics, Sofia University “St. Kliment Ohridski” (FMI-SU) and the Institute of Mathematics and Informatics, BAS (IMI-BAS) in cooperation with the European Consortium for Mathematics in Industry (ECMI). The ESGI'113 was the third Study Group in Bulgaria, after the very successful ESGI'104, September 23–27, 2014 and ESGI'95, September 23–27, 2013.

ESGI'113 was financially supported by the project Advanced Computing for Innovation (ACoIn) funded by FP7 Capacity Programme, Research Potential of Convergence Regions under the grant agreement 316087/2012, and by the Sofia University grant N075/2015. The event was also sponsored by the companies that posed problems for solving, as well as by the project “Supercomputing Expertise for Small and Medium Enterprise Network”, (SESAME-NET), funded by the EU's Horizon 2020 research and innovation programme under grant agreement 654416.

ESGI'113 was hosted by the Institute of Information and Communication Technologies, BAS, and by the Institute of Mathematics and Informatics, BAS. The two institutions have provided excellent conditions for work.

Study Groups with Industry are an internationally recognized method of technology transfer between academia and industry. These one-week long workshops provide an opportunity for engineers and industrial developers to work alongside academic mathematicians, students, and young professional mathematicians on problems of direct practical relevance.

The Organizing Committee selected six problems to work on:

1. *Spline intersection improvement*, Chaos Group Ltd.;
2. *Development of mathematical algorithm for direct ascription of missing values in survey research data*, GemSeek;
3. *Optimal Cutting Problem*, STOBET Ltd.;
4. *The 2D/3D Best-Fit Problem*, EngView Systems Sofia;
5. *Analytical solution for consolidation of a soil layer with finite thickness under cyclic mechanical loading*, GEO|RUHR, Germany;

6. *Cyber Intelligence Decision Support in the Era of Big Data*, STEMO Ltd..

Five of the companies are Bulgarian. The founders of the company GEO|RUHR, Germany have had a long time collaboration with the Institute of Mechanics, BAS.

The participants from Bulgaria (42) and from abroad (2) were divided into six groups, each group working as a team on one problem. The Bulgarian participants were from various Academic institutions: FMI-SU; IMI-BAS; ICT-BAS; Plovdiv University; Veliko Tarnovo University; Technical University of Sofia, University of Rousse. The participants from the University of Novi Sad, Serbia and the Ruhr-University Bochum, Germany, made valuable contributions to the work on the problems.

A separate event, Preparatory Modelling Week, was organized this year by FMI, Sofia University, for senior Bachelor students, Master and Doctoral students. It was designed to run back-to-back (07–11.09) with ESGI'113, providing problem-solving experience and a warm-up for the work in the Study Group. All Modelling week attendees were expected to participate at the study group and this really happened. Twelve of the ESGI participants were students: four Doctoral, four Master and four Bachelor students. The Master students were from the FMI Master programs on Computational mathematics and mathematical modelling and Mathematical modelling in economics, evaluated as ECMI Master Programs in Industrial Mathematics, branch Techno-mathematics and Econo-mathematics respectively.

On the last day of the workshop each group made presentation on the progress in solving their problem and on recommended approaches for their further treatment (including generalization, improvements and implementations. The presentations were the basis of the final report which each group has prepared. These were assembled in this booklet to form the Study Group Final Report and to provide a formal record for the work for both the industrial and academic participants.

The description of the problems, the last day presentations and the final reports of each working group are posted on the website of the ESGI'113:

<http://parallel.bas.bg/ESGI113>

As at ESGI'95 and ESGI'104, certificates for participation and for valuable contribution were given to the participants.

The next Bulgarian Study Group is planned to be held in Sofia in the period July 24-28, 2016, immediately after the ECMI Modelling Week'2016, July 17-21.

List of participants

Ana Avdzhieva (Sofia University, FMI)
Assen Tchorbadjieff (IMI, BAS)
Branko Markovic (University of Novi Sad, Serbia)
Cihan Menseidov (University of Ruse)
Detelina Kirova (IMI, BAS)
Dimitar Fidanov (Plovdiv University, FMI)
Dimo Dimov (IICT, BAS)
Doychin Boyadzhiev (Plovdiv University, FMI)
Dragomir Aleksov (Sofia University, FMI)
Eliza Ilieva (Sofia University, FMI)
Galina Lyutskanova (Sofia University, FMI)
Geno Nikolov (Sofia University, FMI)
Georgi Evtimov (UASG)
Hristo Kostadinov (IMI, BAS)
Ivan Georgiev (IMI, BAS / IICT, BAS)
Kiril Alexiev (IICT, BAS)
Kiril Mihaylov (Sofia University, FMI)
Konstantinos Liolios (IICT, BAS)
Lyudmil Yovkov (Sofia University, FMI)
Maria Georgieva (Plovdiv University, FMI)
Maria Dacheva (IMeh, BAS)
Maria Paskova (Sofia University, FMI)
Maroussia Bojkova (Sofia University, FMI)
Michail Todorov (TU, Sofia)
Nadia Zlateva (Sofia University, FMI)
Nikola Naidenov (Sofia University, FMI)
Nina Daskalova (Sofia University, FMI)

Pavel Iliev (Sofia University, FMI)
Pencho Marinov (IICT, BAS)
Plamen Mateev (Sofia University, FMI)
Stanislav Harizanov (IICT, BAS)
Stanislav Stoykov (IICT, BAS)
Stela Zhelezova (IMI, BAS)
Teodora Ivanova (Sofia University, FMI)
Tihomir Ivanov (Sofia University, FMI)
Todor Balabanov (IICT, BAS)
Tomas Barciada (Ruhr-University Bochum, Germany)
Tsvetomir Tsachev (IMI, BAS)
Vasil Kolev (IICT, BAS)
Velislav Bodurov (Sofia University, FMI)
Vencislav Pirinski (TU, Sofia / IICT, BAS)
Venelin Valkov (Plovdiv University, FMI)
Veska Noncheva (Plovdiv University, FMI)
Zlatogor Minchev (IICT, BAS / IMI, BAS)

PROBLEMS

Problem 1. Spline Intersection Improvement

Chaos Group Ltd., www.chaosgroup.com

Yordan Mandzhunkov, yordan.madzhunkov@chaosgroup.com

Company's overview. Chaos Group creates physically-based rendering and simulation software for artists and designers. Founded in 1997, Chaos Group is a Bulgarian company that has devoted the last 18 years to helping artists advance the speed and quality of one of their most important tools. Today, Chaos Groups photorealistic rendering software, V-Ray[®], has become the rendering engine of choice for many high-profile companies and innovators in the design and visual effects industries.

A task that we typically perform is intersection of spline curves with a ray. We already have developed several models how to intersect such primitives with rays. However, we are looking for a way to improve our current model in terms of accuracy, without sacrificing too much computation speed.

Problem. We model spline curve primitives with 4 control points in 3D space – $p_0; p_1; p_2; p_3$. Each control point has it's own width of the curve – $w_0; w_1; w_2; w_3$. Spline curve center as function of curve's evolution parameter $u \in [0, 1]$ is described with

$$(1) \quad \vec{p}(u) = \vec{p}_3 u^3 + 3\vec{p}_2 u^2(1-u) + 3\vec{p}_1 u(1-u)^2 + \vec{p}_0(1-u)^3.$$

The width of the primitive as function of the same evolution parameter is given by:

$$(2) \quad w(u) = w_3 u^3 + 3w_2 u^2(1-u) + 3w_1 u(1-u)^2 + w_0(1-u)^3.$$

The point that lies on the surface of the primitive has to satisfy the system:

$$(3) \quad \begin{aligned} |\vec{s}(u) - \vec{p}(u)|^2 &= w(u)^2 \\ (\vec{s}(u) - \vec{p}(u)) \cdot \frac{d\vec{p}(u)}{du} &= 0. \end{aligned}$$

For a given ray

$$(4) \quad \vec{r}(t) = \vec{o} + t\vec{d}$$

find $t > 0$ and $u \in [0, 1]$ such that

$$(5) \quad \vec{r}(t) = \vec{s}(u).$$

In case of multiple solutions, we are only interested in the one that has minimum t . We are interested in numerical method that is programmable in c++ and can find accurate solution at the lowest computational cost.

Motivation. The spline curve primitives we described above are widely used for hair in V-Ray. In scene that has one human like character there are typically several million hair strands. Each hair can be composed by many spline primitives. Therefore we need to be able to intersect hair as fast as possible. We have already implemented acceleration data structures as bounding volume hierarchy (BVH) and k-d tree to accelerate intersection. We will use the spline intersection method that you provide, as last phase of the intersection process – after the ray already intersected the bounding box of the spline. We also included a rendered image using our current intersection model:



Problem 2. Development of Mathematical Algorithm for Direct Ascription of Missing Values in Survey Research Data

GemSeek, www.gemseek.com

Martin Dimov, martin.dimov@gemseek.com

Company's overview. GemSeek is a market intelligence and consulting company. It helps business leaders with decision support analytics that have a direct impact on bottom line and competition. Company's services are organized around Data science and predictive analytics, Market & Industry Intelligence, Customer Insight & Brand Analytics, Advanced Visualization Solutions and Competitive Intelligence.

Definition of the problem. One of Gemseek's core activities is developing and implementing marketing survey research studies among different target groups both on local market and across the world. The results serve as basic foundation for further analysis on customer perceptions, behavior and brand affiliation. Hence, the necessity of complete datasets is a prerequisite for sustainable analyses, robust analytics and unbiased interpretation of results. One of the biggest challenges for company was dealing with "blank spots" in the data i.e. places where respondents refrain from providing correct answering due to various reasons. Some of these include difficulty to find correct answer, too long questionnaires, unwillingness to disclose sensitive personal information (income, age etc.), too many options to choose from etc.

Since most statistical analysis methods assume the absence of missing data and are only able to include observations in which every variable is measured, GemSeek is in need of a robust mathematical approach that could impute incomplete data sets so that analyses which require complete observations can appropriately use all the information present in a dataset without missingness. In this case the level bias and incorrect uncertainty estimates will be avoided.

Task description. In 2014 the company has performed a study among 600 customers of the biggest supermarket chains in Bulgaria. The methodology used

random sampling procedure among population in Bulgaria's top 8 cities. The variables were measured with different type of scales: nominal, ordinal and continues in some of the cases. As a result the final dataset contained a large number of missing cases and "no answers" across variables ranging from 5% to around 50% of all respondents interviewed.

Since all methods for stimulating response rate were exhausted GemSeek is looking for a **computational algorithm** that could use the information from already completed cases and recursively assign values to missing data in every variable controlling for the type of scale and distribution of "real" values. For this exercise we assume that all missing values are of type: Missing At Random (MAR).

Expected results

- Brainstorm on various methods of solving the task;
- Presentation of different algorithms, stating pros and cons for each one;
- Used variables, predictors, distance measures, parameter estimates etc.;
- Suggestions of appropriate software and tools, complete scripts and developer codes for completing the task;
- Discussion of the results with bigger audience.

Assessment criteria. All suggestions for algorithms will be closely reviewed and assessed by Gemseek team. Following criteria will be used when choosing the most effective method:

- Accuracy – measured as percentage of accurately imputed cases vs. real cases;
- ROC curves and Confusion matrices – as a way of graphical visualization of accuracy;
- AIC and BIC – as a method for comparing different methods and their efficiency;
- Statistical significance and hypothesis testing – as non-parametric estimation of results.

Materials provided

- Incomplete data set of survey results in CSV format which could be used for imputation methods and comparing the results;
- Complete questionnaire containing names and labels of all variables in the dataset.

Other information and resources and consultations will be readily available from Gemseek team on request.

Problem 3. Optimal Cutting Problem

STOBET Ltd., www.stobet.com

eng. Georgi Evtimov

Company's overview. STOBET is a structural engineering bureau that was set up in 2003 in the city of Sofia by Georgi Evtimov Evtimov. Since its very start the bureau has been dealing with structural design of buildings and facilities. The bureau designs a variety of structures: reinforced concrete, metal, wood and – recently quite often – combined types of structures: steel and reinforced concrete, metal and wood. Combined structures provide very flexible and cheap solutions.

Definition of the problem. Making the project by part “Constructions” contains many drawings. Plotting the project – drawing by drawing – is a laborious work, which is repeated for each printing. The number of drawings can reach 700-800 numbers in one project. For this reason it is necessary to arrange all “small” drawings in the “big” paper in the plotter with a minimum wastage of paper.

Task for optimization

Task 1. We have a large piece of paper $X = 1000$ mm, $Y = 15000$ mm. In this paper many small rectangles (drawings) with dimensions (a_i, b_i) , $i = 1, \dots, n$ should be arranged (see Fig. 1). The goal is to arrange the rectangles in such a way that they fill the entire width of the paper (1000 mm) and use the least possible length of the sheet (i.e. the rectangle that contains all the small drawings has the least possible length). In the process of arranging the “small” rectangles (drawings) can be rotated at any angle (0, 90, or any).

Task 2 (Linear cutting). We have in stock N pieces of rods with section X and length L meters. After the design is given, we need to obtain M_j rods with section X and lengths P_j meters, $j = 1, \dots, m$. The question is how to combine the rods available so that the minimum possible spolage is obtained.

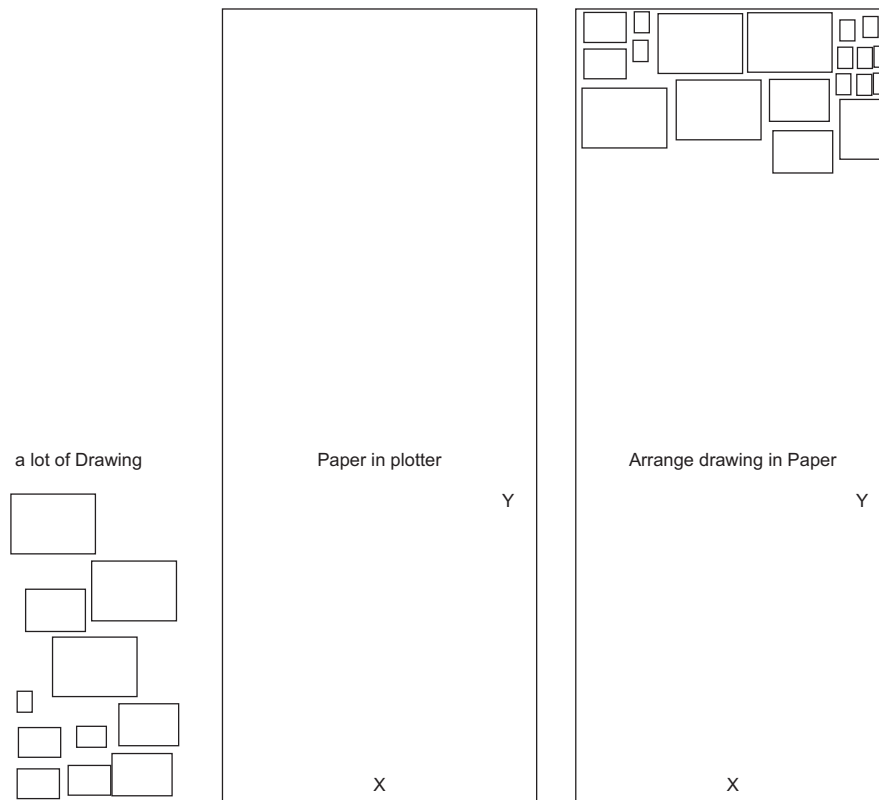


Fig. 1

Example

We have in stock $N = 12$ pcs with section $X = \text{IPE200}$ and length $L = 12000$ mm.

After the design we have to obtain $M = M_1 + M_2$ profiles with section $X = \text{IPE200}$:

1. $M_1 = 18$ pcs with length $P_1 = 7350$ mm,
2. $M_2 = 53$ pcs with length $P_2 = 121$ mm.

The width of cut is 5 mm.

Problem 4. The 2D/3D Best-Fit Problem

EngView Systems Sofia (A Sirma Group Company), www.engview.com

eng. Peter Konyarov, Peter.Koniarov@sirma.bg

Company's overview. Sirma Group Holding JSC is one of the largest software groups in Southeast Europe, with a proven track record since 1992. The group employs more than 300 experienced software professionals who have implemented hundreds of successful projects worldwide.

Sirma has gained substantial expertise in some of the most innovative areas of ICT: semantic technologies, mobile applications, ERP (Enterprise Resource Planning), BI (Business Intelligence), financial, banking and payment services, e-government and others. Our successful projects laid the foundation of the long-term customer relationships. Following its visionary mission, our company has focused on the creation of new knowledge enterprises. A few of Sirma subsidiaries are among the world leaders in their verticals.

The Group traditionally launches innovative businesses; it founded its own business incubator for technology startups a few years ago. Our companies have won many international and national awards. For instance, Sirma Solutions JSC was awarded the Forbes Business Awards 2012 in "Business Development" category; Ontotext won the Innovation Enterprise Award 2014 in the category "Innovation Visionary", the prize of the 3rd NewsHack2014 contest on the BBC. Sirma Mobile JSC was honoured with the prestigious prize for mobile security SIMagine 2011. Sirma Business Consulting JSC was distinguished twice for the Best ICT employer for 2014 and 2012. EngView Systems Jsc, our subsidiary company for CAD/CAM software, was awarded with the European Information Technology Prize.

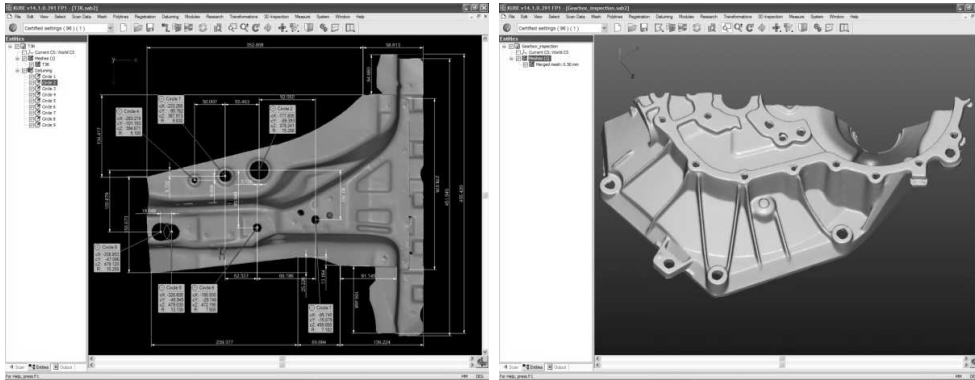
Problem description. In computer systems, the best-fit problem can be described as a search for the best transformation matrix to transform input measured points from their coordinate system into a CAD model coordinate system using a criteria function for optimization. For example, if the criterion is Minimum Sum of Deviations, we search for a transformation matrix M that minimizes the sum of all distances from an matrix-transformed measure points to a CAD model.

The formula that describes this process is as follows:

$\sum_{i=1}^n \text{dist}(Pi.M, CAD\text{surface}) \rightarrow 0$, where n is the number of points and $Pi.M$ is the matrix-transformed measured input point.

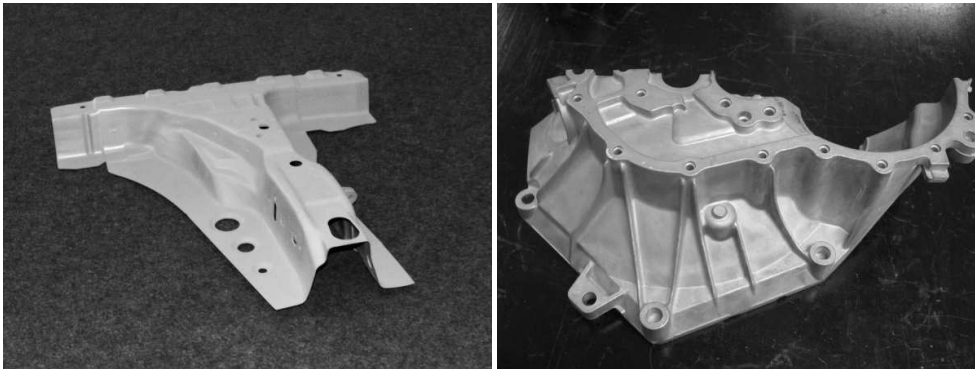
The case. The standard case where the problem takes place is quality control of part production. The process is as follows:

1. Engineers create a part as a CAD model in the coordinate system A (Pic 1).



Pic 1. The CAD model is in the coordinate system A

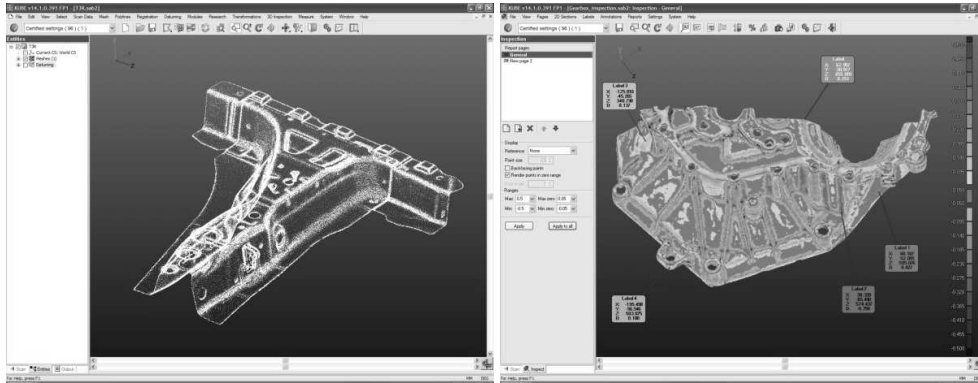
2. The part is produced and is measured as a real-point cloud in the coordinate system B (Pic 2).



Pic 2. The physical part is scanned in the coordinate system B as a points cloud or as a triangular mesh

3. The best-fit matrix allows the direct comparison of the produced part surface relative to the wanted design. After the produced part has been compared with the designer project, it either:

- Passes quality inspection and becomes part of a product, or
- Does not pass quality control, and as a result is discarded.



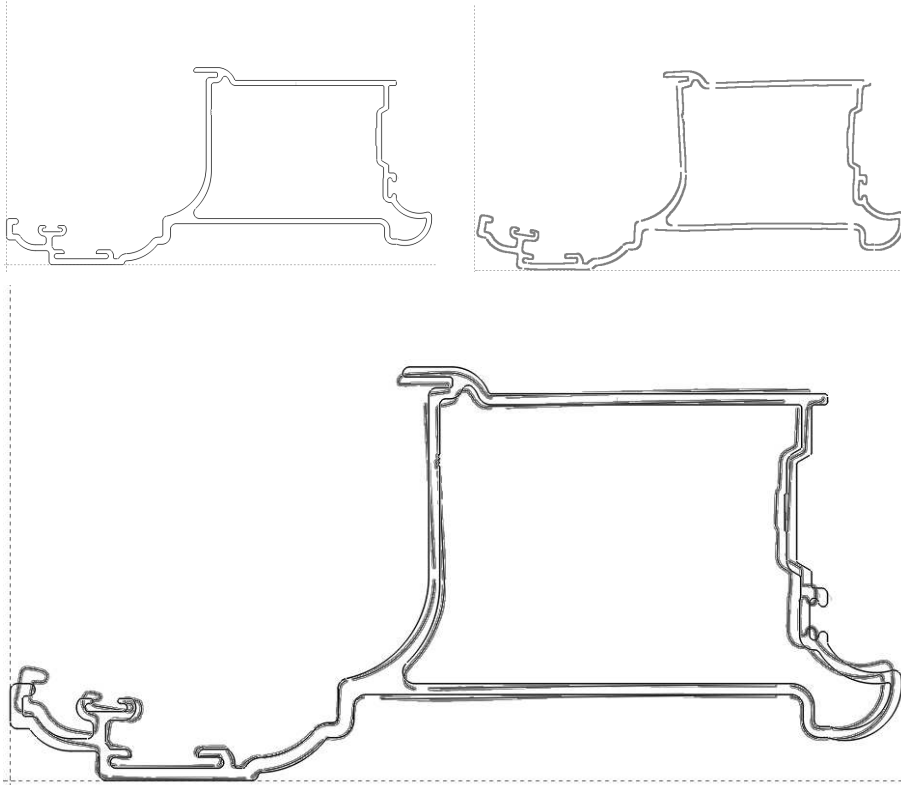
Pic 3. We search for the best transformation that will transform points from coordinate system B to coordinate system A

The solution. The best algorithmic solution should include the following features:

1. Partial fit (only part of the object is scanned).
2. Different parts (these could also be measure points) can have their own individual weights.
3. Only some of the three rotations and three translations can be applicable.
4. The algorithm can be applied on 2D or 3D data.
5. Preliminary assessment can be made if there are points that constitute noise. If such points are detected, they should be filtered out.
6. In the ideal case, the algorithm's input data – these are the data in the two coordinate systems – can appear as points, as a mesh, or as a CAD model.
7. Optimization can take place by different optimization criteria: least squares, minimum sum of deviations, mini-max, uniform deviations, minimum standard deviation, tolerance envelope, tolerance envelope mini-max.
8. The fit process should be able to accept also partially deformed parts. Even if there are discrepancies between the CAD model and the input data, the algorithm must be able to process them.
9. The computation needs to be fast and efficient.

10. An option could exist for multi-core, parallel computation.

2D example:



Problem 5. Analytical solution for consolidation of a soil layer with finite thickness under cyclic mechanical loading

GEO|RUHR, Germany

Thomas Barciaga, Nina Müthing

1. Introduction. GEO|RUHR is a start-up in the field of geotechnical engineering. Among others we offer technology and scientific consultancy for the design of foundations of engineering structures. One of our business segments is the experimental and numerical subsoil analysis. In this framework we experimentally determine and evaluate soil parameters, which are necessary for the assessment of the subsoil behaviour as well as for the numerical modelling of foundation systems. Thereby, GEO|RUHR sets a focus on the analysis of engineering structures founded in soft soils under cyclic loading – e.g. foundation systems for on- and offshore wind turbines – as these systems are gaining increasing attention within the geotechnical community.

2. Objective. When founded on soft cohesive soils pore water dissipation and time evolution of settlements is a key issue in the analysis of relevant foundation systems, as these soils due to their low permeability show a retarded settlement behaviour. In order to do settlement and/or time prognoses for cyclically loaded foundation constructions an exact knowledge of the evolution of pore water pressure dissipation is important. For static loading this problem has been solved for many decades (see Terzaghi, 1923). However, for cyclic load applications as they can be found in the framework of on- and offshore foundation design this problem is not solved completely. By an experimental testing series GEO|RUHR is already able to do prognoses for the pore water dissipation behaviour. However, a comparison of the experimental data to an analytical solution of the consolidation equations is needed to validate the experimental testing results. This is requested as besides numerical methods, analytical solutions are strongly requested to verify the FEM results.

3. Mathematical Problem. An analytical solution for the consolidation process under cyclic loading exists in literature (see e.g. Barends, 2006, 2011).

However, this approach assumes non-realistic boundary conditions as a soil stratum with infinite depth or a layer of high thickness are treated.

Therefore, a solution for a finite soil stratum, or shallow depth (see Fig 1) characterised by the following parameters is to be derived:

- H thickness of the stratum
- k hydraulic permeability of the soil
- K_s bulk modulus
- α compressibility of the solid phase
- β compressibility of the fluid phase
- n porosity
- γ volumetric gravity of the fluid phase

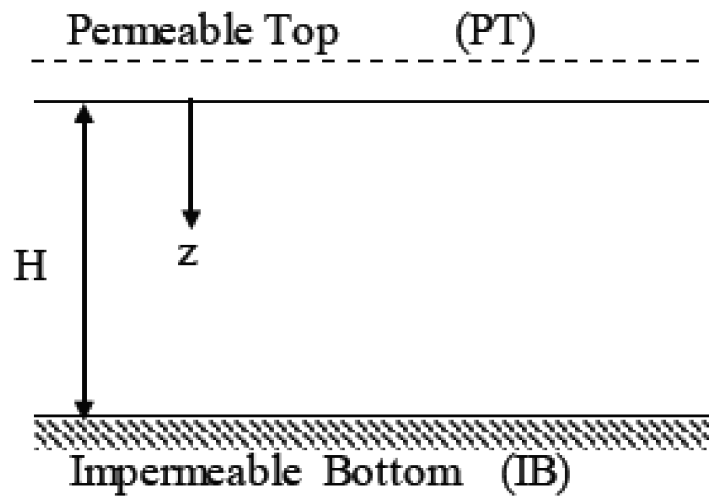


Figure 1. Soil stratum with given boundary conditions (permeable top, impermeable bottom – PTIB)

A vertical, cyclic load is applied to the top of the stratum, e.g. as haversine function of time or other:

$$L(t) = q \sin^2\left(\frac{\pi t}{d}\right) \quad \text{or} \quad L(t) = q \cos\left(\frac{\pi t}{d}\right),$$

where

- $L(t)$ loading function
- t time
- q load amplitude
- d load period

The one-dimensional consolidation equation is given by

$$\frac{\partial u}{\partial t} = C_z \cdot \frac{\partial^2 u}{\partial z^2} + \frac{\alpha}{\alpha + n\beta} \cdot \frac{dL(t)}{dt}.$$

This equation describes the behaviour of the excess pore water pressure u with time and along the depth z . The consolidation coefficient C_z is given as:

$$C_z = \frac{k \cdot K_s}{\gamma(1 + \frac{n\beta}{K_s})}.$$

The boundary conditions may be given as follows

$$u(0, t) = 0, \quad \frac{\partial u}{\partial z}(H, t) = 0.$$

The initial condition is given as

$$u(z, 0) = 0.$$

The task is to find an analytical solution to the above formulated boundary value problem. Next, based on the analytical solution to evaluate the following sub-tasks:

1. excess pore water pressure as a function of time and depth $u(z, t)$;
2. explicitly derive the phase shift ψ between excess pore water pressure $u(z, t)$ and the applied load with time (for a fixed depth) especially at the bottom ψ ($z = H, t \rightarrow \infty$), the phase shift or lag is a positive or negative delay of the excess pore water pressure as compared to the applied surface load that may vary with depth;
3. parameter analysis for the solution regarding permeability k as a function of relevant parameters (stratum height H , bulk modulus K_s , phase shift (see 2.), load amplitude q and loading period d).
4. parameter analysis for the phase shift ψ as a function of the fluid and solid phase compressibility and soil permeability.

Problem 6. Cyber Intelligence Decision Support in the Era of Big Data

STEMO Ltd., <http://www.stemo.bg/>

Georgi Dukov, Georgi_Dukov@stemo.bg

Company's overview. In 2016 STEMO Ltd. is going to celebrate 25 years anniversary with confirmed leading role in the field of information technologies. The company is providing a broad portfolio of IT products, solutions and services to our customers for building and enhancing the efficiency, productivity, security and reliability of their IT infrastructure.

Our versatile professional experience and expertise allow successful implementation of complex projects covering the complete life-cycle of each information system: **consultations, research, analysis, design, planning, implementation, training, operation, optimization, maintenance and upgrade.**

The company has 15 own commercial offices, service and retail centers, warehouses, a training center, equipped with modern information, technological and transport facilities. The branches of the company are situated in the largest cities of Bulgaria.

We employ 260 highly-qualified specialists: sales and technical consultants, service engineers, designers, programmers, economists, etc. with over 600 technical and sales certificates which cover the certification programs of leading world manufacturers.

Our main activities are encompassing almost all services, products and solutions in the field of information technologies, including:

- design, building and maintenance of complex information and communication systems
- delivery and installation of computer and office equipment, software and consumables
- specialized, professional IT services
- warranty and post-warranty support of computer equipment
- software development
- training and certification services

The quality management system of the company was implemented in 2000. It is certified in compliance with the requirements of international standards ISO 9001:2008 and AQAP 2110 NATO standards and covers all branches and activities of the company. The system ensures a high level of customer satisfaction, contributing to the stable development of the company and the fulfillment of corporate objectives. In 2010 the company certified the IT service and information security management according to ISO 20000 and ISO 27000 standards. In 2012 acquired certificates for environmental management ISO 14001 and health and safety management ISO 18001.

The company is a certified direct partner of leading world manufacturers: HP, Microsoft, Cisco Systems, SAP, Oracle, Fujitsu, DELL, Canon, Toshiba, Xerox, Epson, NetApp, VMware, Citrix, D-Link, EATON, APC, Samsung, LG, BenQ, 3M, ESET, Novell, Autodesk, AMP, R&M, Kerpen, Panduit, ITNI, OSPL, Crypto, Systematic, Imanami, Lieberman Softwar, NetSurity, Rola Security Solutions and others.

Our services help customers to achieve maximum return of investments in IT, enhancing the efficiency, productivity, security and reliability of their IT infrastructure. Our customers save time and resources and are able to concentrate on their main activity and priorities.

Over the years, the company financial results have shown a solid development and strengthened our role as an undisputed business leader in the IT market.

The biggest corporate organizations in Bulgaria, state and local administrations, industry and energy enterprises, telecommunication companies, banks, schools and medical centers, NGOs, thousands of SMEs and individuals are among our customers. We stand their success for our own priority.

Every year more than 10 000 organizations and individuals rely on our company as a correct, dedicated and reliable partner.

Problem description. Modern technologies in the digital society are constantly enlarging the cyber space scale, services and capabilities. This opens the necessity for proper understanding the behavior of today's Internet users for assuring a more secure and predictable world. Understanding these evidently requires big data processing and relevant generalization for adequate decision support. STEMO Ltd. is a leading national security systems integrator working in this field since 2009 with multiple successful business partnerships.

Following our practical experience, one of the key problems in the field is to produce a useful aggregation and trends forecasting, in a suitable middleware, concerning the enormous direct and indirect Internet objects relations.

As these generate a number of hybrid threats for the users, critical infrastructure, e-services, AI evolution, M2M autonomous interaction and human-in-the-loop dynamic role, the resulting preventive measures, are quite demanding by means of computational resources and multiple decision makers adequate support.

Being rather comprehensive, the problem requires experts' data combination with big data statistical observations for practical achieving adequate cyber intelligence and countering cybercrimes and terrorist events.

Five key steps for solving the problem could be implemented:

1. Defining multiple cyber risks dynamic database.
2. Formulation of aggregation models, concerning data extraction and visualization.
3. Formulation of discrete optimization problems, taking into account the particular forecasting period, regarding expected critical events.
4. Choosing a software environment for solving the formulated problems.
5. Numerical experiments and discussion of results.

FINAL REPORTS

Spline Intersection Improvement

Dragomir Aleksov, Maria Paskova, Nikola Naidenov, Pencho Marinov

1. Introduction

Rendering and simulation software needs many models of reality. Every human has hair and we need to visualize realistic hair. We can model hair with many spline curves. A typical task of the ray tracing method (see [2]) is finding an intersection of spline curves with a ray. We try to find a fast way to calculate the point where the ray intersects the curve.

Model

- We have to model spline curve primitives with 4 control points in 3D space: $\vec{p}_0; \vec{p}_1; \vec{p}_2; \vec{p}_3$.
- Each control point has its own width of the curve: $w_0; w_1; w_2; w_3$.
- Spline curve center as function of curve evolution parameter is described by

$$\vec{p}(u) = \vec{p}_3 u^3 + 3\vec{p}_2 u^2(1-u) + 3\vec{p}_1 u(1-u)^2 + \vec{p}_0(1-u)^3.$$

- The width of primitive as function of the same evolution parameter is given by:

$$w(u) = w_3 u^3 + 3w_2 u^2(1-u) + 3w_1 u(1-u)^2 + w_0(1-u)^3.$$

The point that lies on the surface of the primitive satisfies the system

$$\begin{cases} |\vec{s}(u) - \vec{p}(u)|^2 = w(u)^2 \\ (\vec{s}(u) - \vec{p}(u)) \cdot \frac{d\vec{p}(u)}{du} = 0. \end{cases}$$

We point out that here $w(u)$ means not the diameter but the radius of the primitive in the point $\vec{p}(u)$.

2. The Problem

Our task is the following:

For a given ray

$$\vec{r}(t) = \vec{o} + t\vec{d}$$

find $t > 0$ and $u \in [0, 1]$ such that

$$\vec{r}(t) = \vec{s}(u).$$

In case of multiple solutions, we are interested in the one that has minimum t .

2.1. Summary of the Report

- We first give an analytical solution of the problem. This leads us to Finding the roots of a function of two arguments.
- If we know that a certain ray intersects a single hair, we propose a simple iterative algorithm to find an approximation of the first point of intersection with any given accuracy.
- Having an iterative algorithm for some good cases we deal with some exceptional ones.
- In the end we consider the problem of whether there is an intersection between a given ray and a certain hair.

Notations

The surface of the hair is given by $\vec{s}(u, v)$ where $u \in [0, 1]$, $v \in [0, 2\pi)$:

$$(2.1) \quad \vec{s}(u, v) = \vec{p}(u) + w(u) \cdot \cos(v) \cdot \vec{a} + w(u) \cdot \sin(v) \cdot \vec{b}.$$

Components of the vectors are:

$$\begin{aligned} \vec{d} &= (d_x, d_y, d_z)^\top, \\ \vec{o} &= (o_x, o_y, o_z)^\top, \\ \vec{p} = \vec{p}(u) &= (p_x, p_y, p_z)^\top, \\ \frac{d\vec{p}(u)}{du} \quad || \quad \vec{q} = \vec{q}(u) &= (q_x, q_y, q_z)^\top, \\ \vec{a} = \vec{a}(u) &= (a_x, a_y, a_z)^\top, \\ \vec{b} = \vec{b}(u) &= (b_x, b_y, b_z)^\top, \\ \vec{r} = \vec{r}(t) &= (r_x, r_y, r_z)^\top, \\ \vec{s} = \vec{s}(u, v) &= (s_x, s_y, s_z)^\top. \end{aligned}$$

Remark 1. The vectors \vec{d} , \vec{q} , \vec{a} , \vec{b} are normed, i.e. $\|\cdot\| = 1$. More, \vec{q} , \vec{a} , \vec{b} are orthogonal and $\vec{b} = \vec{q} \times \vec{a}$. The following rule applies to the selection of \vec{a} :

If $|q_x| \leq \min\{|q_y|, |q_z|\}$ then $\vec{a} = (0, q_z, -q_y)^\top$ and $\vec{b} = (-q_x^2 - q_z^2, q_x q_y, q_x q_z)^\top$;

If $|q_y| \leq \min\{|q_x|, |q_z|\}$ then $\vec{a} = (q_z, 0, -q_x)^\top$ and $\vec{b} = (-q_x q_y, q_x^2 + q_z^2, -q_y q_z)^\top$;

If $|q_z| \leq \min\{|q_y|, |q_x|\}$ then $\vec{a} = (q_y, -q_x, 0)^\top$ and $\vec{b} = (q_x q_z, q_y q_z, -q_x^2 - q_y^2)^\top$;

Remark 2. For the ray $\vec{r}(t)$ and a fixed u we have two cases.

Case 1: If the ray $\vec{r}(t)$ is not parallel to the plane defined by the point $\vec{p}(u)$ and the vector $\vec{q}(u)$ which is orthogonal to this plane (we note that $\vec{q}(u)$ is the tangent of the curve described by the center of the hair $\vec{p}(u)$), then we can calculate

$$(2.2) \quad t = \frac{(\vec{q}(u), \vec{p}(u) - \vec{o})}{(\vec{q}(u), \vec{d})} \quad \text{and,} \quad \vec{r}(t) = \vec{o} + t\vec{d}, \quad \delta = \text{dist}(\vec{r}(t), \vec{p}(u)) - w(u).$$

Case 2: $\vec{d} \perp \vec{q}(u)$ and $(\vec{q}(u), \vec{d}) = 0$, we calculate only $(\vec{q}(u), \vec{p}(u) - \vec{o})$ which gives us the signed distance between the ray and the plane - we need this scalar product to be 0.

Analytical solution of the problem

An intersection between surface $\vec{s}(u, v)$ and the ray $\vec{r}(t)$ happens in a point (u, t) which is a solution of the system:

$$\vec{s}(u, v) = \vec{r}(t)$$

or written in components (u is omitted for simplicity):

$$(2.3) \quad \begin{cases} p_x + w \cdot \cos(v) \cdot a_x + w \cdot \sin(v) \cdot b_x & = & o_x + t \cdot d_x \\ p_y + w \cdot \cos(v) \cdot a_y + w \cdot \sin(v) \cdot b_y & = & o_y + t \cdot d_y \\ p_z + w \cdot \cos(v) \cdot a_z + w \cdot \sin(v) \cdot b_z & = & o_z + t \cdot d_z \end{cases}$$

or equivalently

$$\begin{cases} w \cdot \cos(v) \cdot a_x + w \cdot \sin(v) \cdot b_x & = & o_x + t \cdot d_x - p_x \\ w \cdot \cos(v) \cdot a_y + w \cdot \sin(v) \cdot b_y & = & o_y + t \cdot d_y - p_y \\ w \cdot \cos(v) \cdot a_z + w \cdot \sin(v) \cdot b_z & = & o_z + t \cdot d_z - p_z. \end{cases}$$

After we square and sum up the three equations above we get:

$$\begin{aligned} w^2 \cdot \cos^2(v) \cdot (a_x^2 + a_y^2 + a_z^2) + w^2 \cdot \sin^2(v) \cdot (b_x^2 + b_y^2 + b_z^2) \\ + 2 \cdot w^2 \cdot \cos(v) \cdot \sin(v) \cdot (a_x b_x + a_y b_y + a_z b_z) = \end{aligned}$$

$$\begin{aligned}
&= t^2 \cdot (d_x^2 + d_y^2 + d_z^2) - 2t \cdot ((p_x - o_x) \cdot d_x + (p_y - o_y) \cdot d_y + (p_z - o_z) \cdot d_z) \\
&\quad + (p_x - o_x)^2 + (p_y - o_y)^2 + (p_z - o_z)^2, \\
&\quad t^2 - 2t \cdot \vec{d} \cdot (\vec{p} - \vec{o}) + (\vec{p} - \vec{o})^2 - w^2 = 0.
\end{aligned}$$

We now substitute: $B = \vec{d} \cdot (\vec{p} - \vec{o}) = (\vec{d}, \vec{p} - \vec{o})$, $C = (\vec{p} - \vec{o}, \vec{p} - \vec{o}) - w^2$ and receive the quadratic equation:

$$(2.4) \quad t^2 - 2.B.t + C = 0.$$

The solution depends from

$$(2.5) \quad D = (B^2 - C).$$

If $D > 0$ we have two roots: $t_1 = B + \sqrt{D}$, $t_2 = B - \sqrt{D}$.

If $D = 0$ we have one root: $t_0 = B$.

If $D < 0$ we have no roots.

Let t_0 be a solution of (2.4) and we know $\vec{r}(t_0)$, $\vec{r}(t_0) - \vec{p}(u)$. We have to check whether they are foreign solutions:

Let $\varepsilon > 0$ be some tolerance. If $|(\vec{q}, \vec{r} - \vec{p})| > \varepsilon$ then this t_0 is not a solution of the system (2.3).

Now equation (2.4) is a of the type $F(u, t) = 0$. The highest degree of u is 6 and of t is 2. Since we know that $u \in [0, 1]$ and also know the cuboid which contains the hair primitive (the company that has proposed the problem has information about it), we are able to restrict t within a certain interval $[T_0, T_N]$. This reduces the problem to finding the zeros of the function $F(u, t)$ in the rectangle $[0, 1] \times [T_0, T_N]$, for which we can apply some known algorithm. From the obtained (if any) zeros in that rectangle (which are also a solution of the system (2.3)) we chose the one with the smallest t .

2.2. An iterative method

If we know that there is an intersection between the hair and the ray that we are considering, we divide the interval $[0, 1]$ into N subintervals with the points $u_i = i/N$, $i = 0, \dots, N$. For a fixed u_i we consider the plane that is orthogonal to the vector of the direction $\frac{d\vec{p}(u_i)}{du}$ and passes through the point $\vec{p}(u_0)$. We are interested in the point in which the ray $\vec{r}(t)$ intersects this plane. Let this happen for $t = t_i$. Then the vector $\vec{r}(t_i) - \vec{p}(u_i)$ must be orthogonal to the direction of the curve describing the center of the hair, i.e. we have

$$(\vec{r}(t_i) - \vec{p}(u_i)) \cdot \frac{d\vec{p}(u_i)}{du} = (\vec{o} + t_i \vec{d} - \vec{p}(u_i)) \cdot \frac{d\vec{p}(u_i)}{du} = 0,$$

or equivalently

$$(o_x + t_i d_x - p_x(u)) \frac{dp_x(u)}{du} + (o_y + t_i d_y - p_y(u)) \frac{dp_y(u)}{du} + (o_z + t_i d_z - p_z(u)) \frac{dp_z(u)}{du} = 0,$$

which is a linear equation for t_i . Having the point from the ray $\vec{r}(t_i)$, we calculate how far it is from the point $\vec{p}(u_i)$:

$$|\vec{r}(t_i) - \vec{p}(u_i)|^2 = [t_i d_x - p_x(u_i)]^2 + [t_i d_y - p_y(u_i)]^2 + [t_i d_z - p_z(u_i)]^2.$$

When we have that

$$|\vec{r}(t_{i-1}) - \vec{p}(u_{i-1})|^2 > w(u_{i-1})^2$$

and

$$|\vec{r}(t_i) - \vec{p}(u_i)|^2 < w(u_i)^2$$

for some u_{i-1} and u_i , this means that somewhere between u_{i-1} and u_i (correspondingly t_{i-1} and t_i) the ray intersects the hair. Actually we have to find all such couples of points (u_{i-1}, u_i) and then take the smallest corresponding t_{i-1} and t_i (this is because we may have several intersections and it is possible to have the smallest t for the largest u). Then we can break the interval $[u_{i-1}, u_i]$ into subintervals with the points v_0, \dots, v_{N_1} and repeat the algorithm for the interval $[v_0, v_{N_1}]$ instead of $[0, 1]$. We repeat this algorithm until the distance between $\vec{r}(t_{i-1})$ and $\vec{r}(t_i)$ becomes less than the required accuracy. This approach is being illustrated on Fig. 1 and Fig. 2.

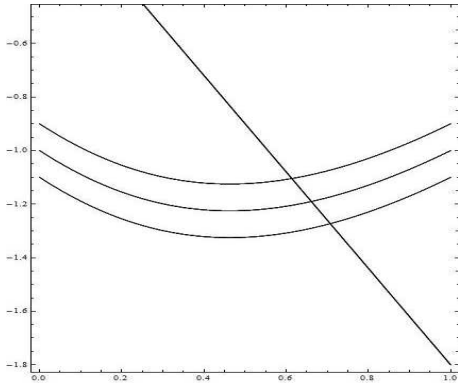


Fig. 1a. The central curve is the center of the hair and the outer are from its surface

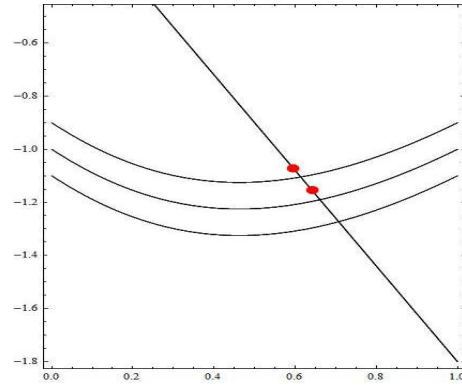


Fig. 1b. We have two points $\vec{r}(t_{i-1})$ and $\vec{r}(t_i)$ from the ray that correspond to two consecutive points from the curve of the center of the hair.

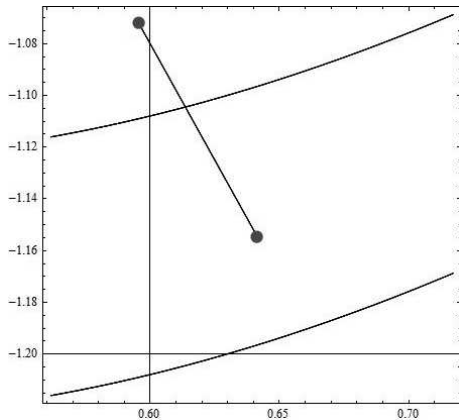


Fig. 2a. Now we consider the part of the ray which is between the points $\vec{r}(t_{i-1})$ and $\vec{r}(t_i)$.

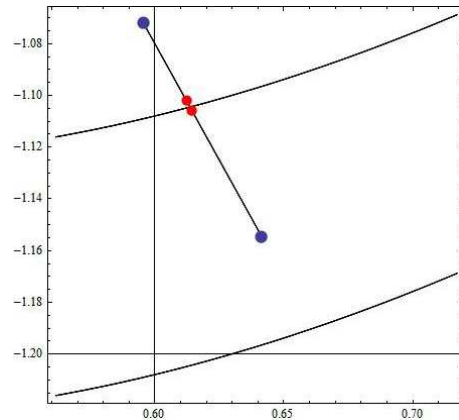


Fig. 2b. We get the two inner points when we apply again our method for the subinterval $[u_{i-1}, u_i]$ which is divided in 10 subintervals.

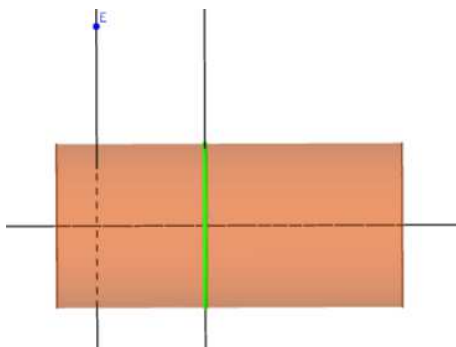


Fig. 3a. The ray is parallel to the plane that passes through $\vec{p}(u)$ and is orthogonal to $\vec{q}(u)$.

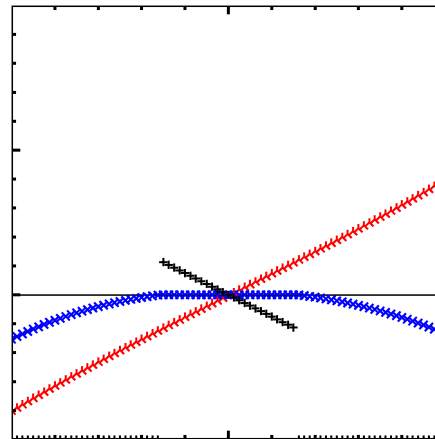


Fig. 3b

2.3. Exceptions

A plane parallel to the ray

A problem with the algorithm described above will occur if the fixed plane through $\vec{p}(u)$ and orthogonal to $\frac{d\vec{p}}{du}(u)$ is parallel to \vec{d} (see Figure 3a). This means that we have $(\vec{q}(u), \vec{d}) = 0$. This case was tackled in case 2 of Remark 2.

A short description of Fig. 3b, Fig. 4b and Fig. 5b

The horizontal axis corresponds to the variable $u \in [0, 1]$. In our numerical experiments the step is 0.005 (see also Section 2.2 for this approach). The vertical axis has several meanings:

- The curve with symbols “X” (blue in color variant) responds to the value D from (2.5) if $D < 0$, and $\text{dist}(\vec{p}(u), \vec{r}(t)) - w(u)$ otherwise, where t is solution of (2.4).

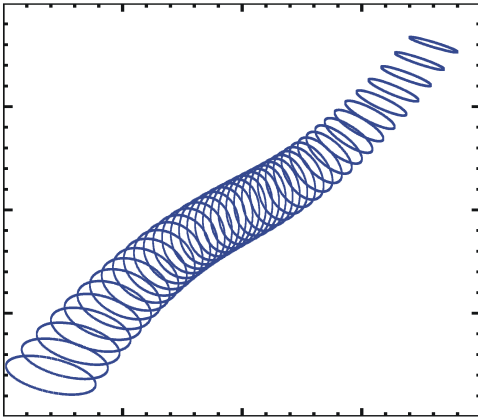


Fig. 4a

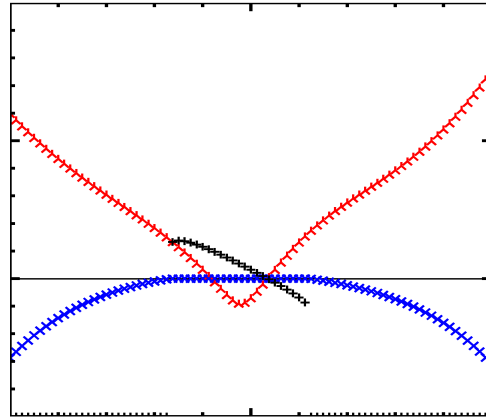


Fig. 4b

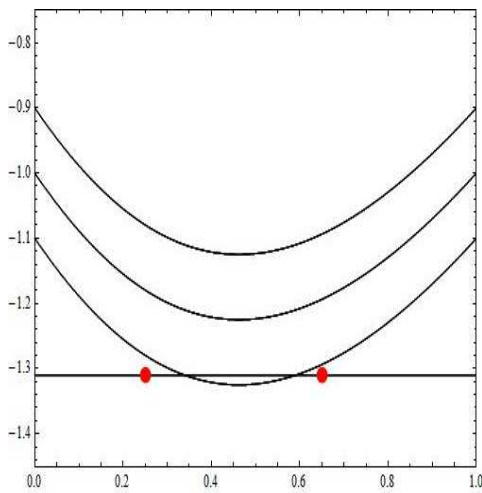


Fig. 5a

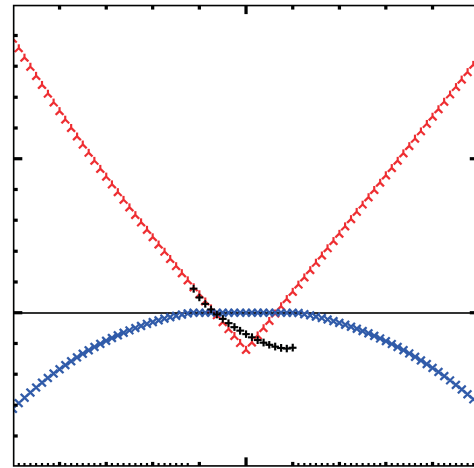


Fig. 5b

- The angled linetype with rotated symbol “Y” (red in color variant) corresponds to the δ from (2.2) in Case 1 of Remark 2 if $(\vec{q}(u), \vec{d}) \neq 0$ and to the value $(\vec{q}(u), \vec{p}(u) - \vec{o})$ from Case 2 of the Remark 2 otherwise.
- The linetype with symbols “+” (black in color variant) is result of checking whether the solution of (2.4) is solution for (2.3), i.e. checking orthogonality of \vec{q} and $(\vec{r} - \vec{p})$.

The range of vertical axis is $[-0.5, 1.0]$ and the horizontal straight line is the zero (i.e. passes through zero).

For the more general case (see Fig. 4a for hair and Fig. 4b for the analysis) for all u the “Y” curve describes the first case of Remark 2. Simultaneously, the localization by proposed method above for the problem (2.3) also works well (see “X” line and short “+” one in the middle on Fig. 4b).

For the special case when the central curve of the hair lies in a plane perpendicular to the ray, then orthogonal planes to the central curve for all u are parallel to the ray (see Fig. 3a), but that does not stop us to locate the intersection of the beam $\vec{r}(t)$ with the surface $\vec{s}(u, v)$. Note that all points from “Y”-curve for Fig. 3b are from second case of Remark 2.

Fig. 5b illustrates another particular case, when the beam pierces the surface near the border at the intersection may be omitted.

How close we are to the intersection? The calculations from Remark 2 give an answer to this question.

When the step is too big

A possible problem when applying the iterative algorithm is when a very little segment of the line described by $\vec{r}(t)$ is in the hair. In such cases it is possible to have two points of the ray $\vec{r}(t_i)$ and $\vec{r}(t_{i+1})$ both of which are outside the hair but between them there is an intersection (see Figure 5a). If we know that there should be an intersection, but we don't find one, we may divide the interval of the parameter u into more subintervals.

Another approach to deal with such cases is to look for “suspicious” points, i.e. points u_i and t_i for which

$$R_i := |\vec{r}(t_i) - \vec{p}(u_i)|^2 - w(u_i)^2$$

is less than a certain (small) value. We will estimate $R_i + R_{i+1}$. The mentioned estimate of $R_i + R_{i+1}$ we calculate when the ray is tangential to the primitive of the hair at one end point for $[u_i, u_{i+1}]$, say u_i . In addition, we assume the maximal perturbation of the axis $p(u)$ in the opposite direction of B_{i+1} (the geometrical

meaning of $B_i = B(u_i)$ is the common point of the ray and the plane through $\vec{p}(u_i)$ and perpendicular to $\vec{q}(u_i)$ and we approximate it by $\frac{1}{2}|p''|h^2$. Similarly, we assume the maximal change of $w(u)$ from its tangent and also approximate it up to second order. Then, for the criterion of this exception we obtain

$$R_i + R_{i+1} < \epsilon, \quad (R_i, R_{i+1} > 0),$$

where

$$\epsilon = h^2[(|\vec{q}| \tan |\varphi| + \frac{1}{2}|\vec{k}|h)^2 + (|\vec{k}| + |w''|)w]$$

with $\vec{q} = \frac{d\vec{p}}{du}(u_i)$ (or u_{i+1}), $\vec{k} = \frac{d^2\vec{p}}{du^2}(u_i)$, $\varphi = \angle(\vec{d}, \vec{q})$, $w = w_i$ (or w_{i+1}) and $w'' = w''(u_i)$.

We see that the probability for this exception is "very small" for "small" h .

2.4. Investigation if the ray intersects the hair

Now we consider the question of whether the ray intersects or not the hair primitive. An important aspect of our approach here is that the company has the information about the cuboid which contains the primitive (Fig. 6). This

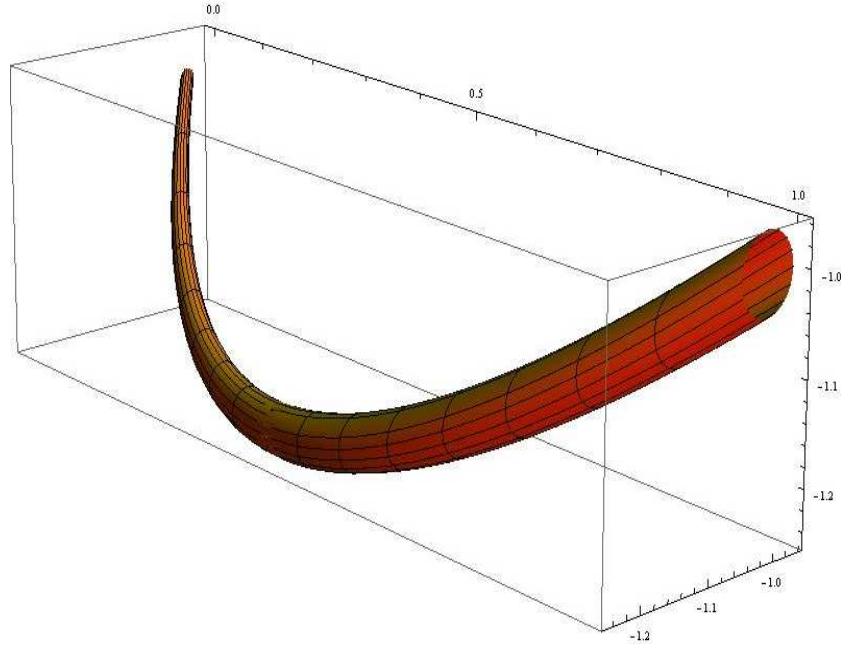


Fig. 6. The cuboid which contains the considered hair primitive is known.

means that we are able to define the interval $[T_0, T_N]$ for which $\vec{r}(t)$ belongs to the cuboid. Without loss of generality we may consider \vec{d} as a unit vector. If the ray intersects the hair then there is a point (u_0, t_0) (many points but one is enough) for which

$$|\vec{o} + t_0\vec{d} - \vec{p}(u_0)|^2 < w(u_0)^2$$

or equivalently

$$|\vec{o} + t_0\vec{d} - \vec{p}(u_0)|^2 - w(u_0)^2 < 0.$$

So, we are interested whether the expression

$$t^2 - 2Bt + C$$

where $B = B(u) = \vec{d} \cdot (\vec{p} - \vec{o}) = (\vec{d}, \vec{p} - \vec{o})$ and $C = c(u) = (\vec{p} - \vec{o}) - w(u)^2$ becomes less than 0 in the rectangle $[0, 1] \times [T_0, T_N]$. This reduces the problem to finding the minimum of a function of two variables t and u – the highest degree of u is 6 and of t is 2. Actually this is the expression obtained when we derived the analytical solution with the difference that here we are interested not in its zeros, but in its absolute minimum.

3. Summary

The problem was to find the first point of intersection (or an approximation of this point) between a ray and a hair in the fastest possible way. We did the following activities:

- found an analytical solution of the problem;
- developed an iterative algorithm for finding the point of intersection (when we know we have one);
- considered some exceptional cases;
- made up an algorithm for finding whether a given ray intersects the hair we are considering.

One can choose from two options: numerically find the zeros (if any) of a function of two variables (one of degree 2 and the other of degree 6) or numerically find its minimum and than (if this minimum is less than zero) use the iterative approach.

Acknowledgments

The first and the third authors were supported by the Sofia University Science Foundation under Project 75/2015. The last author was partially supported by the Bulgarian National Scientific Fund under the grant DFNI I02/05.

References

- [1] G. Stanilov. Analytic Geometry, Publishing House "Science and Art", 1977 (in Bulgarian).
- [2] David F. Rogers. Procedural Elements for Computer Graphics, McGraw Hill, 1998.

Direct Ascription of Missing Categorical Values in Survey Research Data

Vasil Kolev, Veska Noncheva, Venelin Valkov
Elica Ilieva, Maria Dobрева

Abstract

The complete datasets are a prerequisite for sustainable analyses, robust analytics and unbiased interpretation of results. Missing values in a survey occur when no data value is stored for the variable in an observation. Missing data can have a significant effect on the conclusions that can be drawn from the data. Direct ascription is the process of replacing missing data with predicted values. The aim of this work is to describe an approach to direct ascription of missing categorical values in survey research data based both on the assumption that values in a data set are missing at random and on the implementation of the correspondence analysis.

Key words: correspondence analysis, supplementary points

1. Introduction

One of the biggest challenges in marketing survey research studies is dealing with “blank spots” in the data i.e. places where respondents refrain from providing correct answering due to various reasons. Some of these include difficulty to find correct answer, too long questionnaires, unwillingness to disclose sensitive personal information (income, age etc.), too many options to choose from etc.

Since most statistical analysis methods assume the absence of missing data and are only able to include observations in which every variable is measured, every company developing and implementing marketing survey research studies is in need of a robust mathematical approach that could impute incomplete data sets so that analyses which require complete observations can appropriately use all the information present in a dataset without missingness. In this case the level bias and incorrect uncertainty estimates will be avoided.

Until the 1970s, missing values were handled primarily by editing. Rubin developed a framework of inference from incomplete data that remains in use today [7]. The formulation of the expectation-maximization (EM) algorithm made it feasible to compute maximum likelihood (ML) estimates in many missing-data problems [1]. Rather than deleting or filling in incomplete cases, ML treats

the missing data as random variables to be removed from (i.e., integrated out of) the likelihood function as if they were never sampled. Many examples of EM were described by Little and Rubin [4]. Their book also documented the shortcomings of case deletion and single imputation, arguing for explicit models over informal procedures. About the same time, in [8] Rubin introduced the idea of multiple imputation (MI), in which each missing value is replaced by two or more simulated values prior to analysis [3]. Creation of MIs was facilitated by computer technology and new methods for Bayesian simulation discovered in the late 1980s [9]. ML and MI are now becoming standard because of implementation in free and commercial software [10].

2. Definition of the problem

In 2014 a market intelligence and consulting company has performed a study among 600 customers of the biggest supermarket chains in Bulgaria. The methodology used random sampling procedure among population in Bulgaria's top 8 cities. The variables were measured with different type of scales: nominal, ordinal and continues in some of the cases. As a result the final dataset contained a large number of missing cases and "no answers" across variables ranging from 5% to around 50% of all respondents interviewed. Since all methods for stimulating response rate were exhausted the company is looking for a computational algorithm that could use the information from already completed cases and recursively assign values to missing data in every variable controlling for the type of scale and distribution of "real" values. For this study we assume that all missing values are of type: Missing At Random (MAR).

3. Introduction to correspondence analysis

Correspondence analysis (CA) represents yet one more method for analyzing data in contingency tables and can be regarded as a special kind of canonical correlation analysis [2]. The main purpose of CA is to reveal the structure of complex data matrix by replacing the raw data with a more simple data matrix without losing essential information. CA makes it possible to present the results visually, that is, as points within a space, which facilitates interpretation. CA is a method especially for analysis of large contingency tables. The technique is a tool to analyze the association between 2 or more categorical variables by representing the categories of the variables as points in 2D or 3D.

Correspondence analysis was developed in France and is more commonly used in Europe than in North America. Correspondence analysis is a descrip-

tive/exploratory technique designed to analyze two-way and multi-way tables containing measures of correspondence between the row and column variables. The results produced by correspondence analysis provide information which is similar to that produced by principal components or factor analysis. They allow one to explore the structure of the categorical variables included in the table. Correspondence analysis seeks to represent the relationships among the categories of row and column variables with a smaller number of latent dimensions. It produces a graphical representation of the relationships between the row and column categories in the same space.

Correspondence analysis was initially proposed as an inductive method for analyzing linguistic data. From a philosophy standpoint, correspondence analysis simultaneously processes large sets of facts, and contrasts them in order to discover global order; and therefore it has more to do with synthesis (etymologically, to synthesize means to put together) and induction. On the other hand, analysis and deduction (viz., to distinguish the elements of a whole; and to consider the properties of the possible combinations of these elements) have become the watchwords of data interpretation. It has become traditional now to speak of data analysis and correspondence analysis, and not data synthesis or correspondence synthesis.

Correspondence analysis is applied to two-way tables of counts. CA can be seen as a special case of canonical correlation analysis. It seeks scores for the rows and columns which are maximally correlated. As in principal component analysis, the aim of correspondence analysis is to reduce the dimensionality of a data matrix in order to visualize it in a subspace of low dimensionality, commonly two- or three- dimensional ([2], [5], [6]).

To summarize the theory of CA, first divide the $\mathbf{I} \times \mathbf{J}$ data matrix, denoted by \mathbf{N} , by its grand total n to obtain the so-called correspondence matrix $\mathbf{P} = \mathbf{N}/n$. Let the row and column marginal totals of \mathbf{P} be the vectors \mathbf{r} and \mathbf{c} respectively, that is the vectors of row and column masses $\mathbf{r} = \mathbf{P}\mathbf{1}$, $\mathbf{c} = \mathbf{P}^\top\mathbf{1}$, where the notation $\mathbf{1}$ is used for a vector of ones of length that is appropriate to its use. Let $\mathbf{D}_r = \text{diag}(\mathbf{r})$ and $\mathbf{D}_c = \text{diag}(\mathbf{c})$ be the diagonal matrices of row and column masses.

The computational algorithm to obtain coordinates of the row and column profiles with respect to principal axes, using the singular-value decomposition (SVD), is as follows:

- (1) Calculate the matrix of standardized residuals: $\mathbf{S} = \mathbf{D}_r^{-\frac{1}{2}}(\mathbf{P} - \mathbf{rc})\mathbf{D}_c^{-\frac{1}{2}}$.
- (2) Calculate the SVD: $\mathbf{S} = \mathbf{U}\mathbf{D}_\alpha\mathbf{V}^\top$, where $\mathbf{U}^\top\mathbf{U} = \mathbf{V}^\top\mathbf{V} = \mathbf{I}$.

(3) Principal coordinates of rows: $\mathbf{F} = \mathbf{D}_r^{-\frac{1}{2}} \mathbf{U} \mathbf{D}_\alpha$.

(4) Principal coordinates of columns: $\mathbf{G} = \mathbf{D}_c^{-\frac{1}{2}} \mathbf{V} \mathbf{D}_\alpha$.

(5) Standard coordinates of rows: $\mathbf{X} = \mathbf{D}_r^{-\frac{1}{2}} \mathbf{U}$.

(6) Standard coordinates of columns: $\mathbf{Y} = \mathbf{D}_c^{-\frac{1}{2}} \mathbf{V}$.

The total variance of the data matrix is measured by the inertia which is calculated on relative observed and expected frequencies.

The rows of the coordinate matrices in (3)–(6) above refer to the rows or columns of the original table. The columns of these matrices refer to the principal axes, or dimensions, of the solution. The row and column principal coordinates are scaled in such a way that $\mathbf{F} \mathbf{D}_r \mathbf{F}^\top = \mathbf{G} \mathbf{D}_c \mathbf{G}^\top = \mathbf{D}_\alpha^2$. The standard coordinates have weighted sum-of-squares equal to 1: $\mathbf{X} \mathbf{D}_r \mathbf{X}^\top = \mathbf{Y} \mathbf{D}_c \mathbf{Y}^\top = \mathbf{I}$.

Package *ca* in R implements CA. The output of function *ca()* is structured as a list-object. The *ca()* output contains the eigenvalues and percentages of explained inertia for all possible dimensions. Values for the rows and columns (masses, chi-squared distances of points to their average, inertias and standard coordinates) are also given.

Eigenvalues and relative percentages of explained inertia are given for all available dimensions. Additionally, cumulated percentages and a scree plot are shown. The items given in rows and columns of *summary()* include the principal coordinates for the first two dimensions ($k = 1$ and $k = 2$). Squared correlations and contributions for the points are displayed next to the coordinates. Notice that the quantities in these tables are multiplied by 1000 (e.g., the coordinates and masses).

The rows and columns of a data table analyzed by CA are called active points. These are the points that determine the orientation of the principal axes.

It happens that there are additional rows and columns of data that are not the primary data of interest but that are useful in interpreting features discovered in the primary data. Any additional row or column of a data matrix can be positioned on an existing map. These additional rows or columns that are added to the map are called supplementary points.

Supplementary variables have no impact on the computation. They are projected onto the solution space afterwards. Thus, contributions are not applicable for this case. Squared correlations as a measure of how well a point is represented

by the axes are still meaningful for the case of supplementary variables and thus are included in the output.

The results from CA can be visualized in the following way. The graphical solution can be restricted to two dimensions—first principal axis to be displayed horizontally (the x-axis) and the second principal axis to be displayed vertically (the y-axis). Usually the first two dimensions are plotted. However, eigenvalues are known for all possible dimensions. The supplementary variables can be added to the plot with a different symbol.

A three-dimensional display of the CA can also be created. This type of display offers the advantage that one can zoom and navigate using the mouse.

4. Results from CA

CA is performed on the provided survey dataset from GemSeek, Bulgaria. For this aim a data submatrix without missing data is extracted. This matrix contains 264 rows and 4 columns.

The shopping behavior is cross-tabulated according to how often clients shop food and grocery products in supermarket (six levels: daily, OnceTwiceAWeek, OnceEveryFewDays, OnceEvery2-4weeks, OnceEvery1-3months, OnceEvery3-6months) and most important factors for clients when deciding from which hypermarket to shop from (16 levels). The contingency table is reproduced in Table 1.

In Table 2 two supplementary rows are added. First supplementary row is “household’s monthly combined income” and it contains five possible answers (Less5K, 5K-10K, 10K-15K, 15K-20K, 25K-30K, MoreThan30K, IDoNotWant-ToDeclare). Second supplementary row is the age with the following levels: 20-24, 25-29, 30-34, 35-39, 40-44, 45-50.

One cannot visualize the profiles exactly, since they are points situated in a four-dimensional space. CA identifies a low-dimensional subspace, which approximately contains the profiles. It reduces the dimensionality of the cloud of points so that we can visualize their relative positions. However, CA gives the coordinates of row and column points for all possible dimensions. This gives us the key to the interpretation of the association between the points.

The algorithm for direct ascription of missing categorical values is based on the association between levels of categorical variables. All associations deduced in this task are presented in Table 3, Table 4, and Table 5.

Table 1. Contingency table with active points

	1	2	3	4	5	6	7	8	9	10	11	12	13	14	15	17
daily	15	3	9	9	9	11	4	4	8	8	4	3	2	2	3	2
OnceEvery1-3months	1	0	0	0	0	1	0	0	0	0	0	0	0	0	0	0
OnceEvery2-4weeks	6	3	0	3	1	3	5	1	0	0	0	0	1	1	0	0
OnceEvery3-6months	0	0	0	0	0	0	0	0	1	0	0	0	0	0	1	0
OnceEveryFewDays	11	4	4	8	10	13	4	11	6	8	0	3	0	1	0	0
OnceTwiceAWeek	7	7	5	5	6	4	6	3	2	3	2	4	2	1	0	0

Table 2. Contingency table with active and supplement points

	1	2	3	4	5	6	7	8	9	10	11	12	13	14	15	17
10K-15K	6	2	3	5	7	4	3	1	2	1	1	2	1	1	0	1
15K-20K	1	1	2	1	0	1	1	0	1	0	1	0	0	0	1	0
25-29	7	2	1	7	2	14	2	1	2	6	1	3	2	2	1	0
25K-30K	1	0	0	0	0	0	0	0	0	0	0	0	0	0	0	0
30-34	11	6	4	6	6	4	4	5	4	2	0	1	2	0	1	1
35-39	6	3	5	4	7	8	4	2	4	2	0	1	0	1	1	0
40-44	8	3	6	4	9	1	6	5	3	4	2	3	1	1	1	1
45-50	8	3	2	4	3	5	3	6	3	5	3	2	0	1	0	0
5K-10K	21	5	4	13	15	8	11	11	8	13	3	4	0	3	2	0
daily	15	3	9	9	9	11	4	4	8	8	4	3	2	2	3	2
IDoNotWantToDeclare	4	5	5	1	4	5	2	3	1	3	0	2	1	0	1	1
Less5K	7	4	4	5	1	13	2	4	4	2	2	1	3	1	0	0
MoreThan30K	0	0	0	0	0	1	0	0	0	0	0	0	0	0	0	0
OnceEvery1-3months	1	0	0	0	0	1	0	0	0	0	0	0	0	0	0	0
OnceEvery2-4weeks	6	3	0	3	1	3	5	1	0	0	0	0	1	1	0	0
OnceEvery3-6months	0	0	0	0	0	0	0	0	1	0	0	0	0	0	1	0
OnceEveryFewDays	11	4	4	8	10	13	4	11	6	8	0	3	0	1	0	0
OnceTwiceAWeek	7	7	5	5	6	4	6	3	2	3	2	4	2	1	0	0

We have detected strong connection between the following levels (see Table 3):

- Level 30-34 of Q2 (How old are you?) and level 4 (Brands available) of Q9.
- Level 25-29 of Q2 (How old are you?) and level 6 (Store spaciousness and organization) of Q9.

It means that if in an observation the level of Q9 is missing (NA) and the level of Q2 is 30–34 then NA values of Q9 can be estimated (imputed) by value 4 (Brands available) and vice versa – the missing values of Q2 can be estimated by 30-34 when the value of Q9 is 4. If the level of Q9 is missing (NA) and the level of Q2 is 25-29, then NA values of Q9 can be estimated by value 6 (Store spaciousness and organization) and vice versa.

Table 4 and Table 5 present the following possible imputations:

- If the level of Q9 is missing (NA) and the level of Q28 is 5 000-10 000, then NA values of Q9 can be estimated (imputed) by value 4 (Brands available) and vice versa.

Table 3. Relationships between some levels of Q2 and Q9

Q2: How old are you?	Q9: Which of these factors is most important to you when deciding from which hypermarket to shop from?
30-34	4 (Brands available)
25-29	6 (Store spaciousness and organization)

Table 4. Relationships between some levels of Q28 and Q9

Q28: What is your households monthly combined income?	Q9: Which of these factors is most important to you when deciding from which hypermarket to shop from?
5 000-10 000 HRK	4 (Brands available)

Table 5. Relationship between some levels of Q4 and Q9

Q4: How often do you shop food and grocery products in supermarket/hypermarket?	Q9: Which of these factors is most important to you when deciding from which hypermarket to shop from?
daily	9 (Product promotions like buy one get one free)
OnceTwiceAWeek	2 (Diversity of goods sold in the store)
OnceEveryFewDays	8 (Benefits from loyalty program)

- If the level of Q9 is missing (NA) and the level of Q4 is daily, then NA values of Q9 can be estimated (imputed) by value 9 (Product promotions like buy one get one free) and vice versa.
- If the level of Q9 is missing (NA) and the level of Q4 is OnceTwiceAWeek, then NA values of Q9 can be estimated (imputed) by value 2 (Diversity of goods sold in the store) and vice versa.
- If the level of Q9 is missing (NA) and the level of Q4 is OnceEveryFewDays, then NA values of Q9 can be estimated (imputed) by value 8 (Benefits from loyalty program) and vice versa.

New data submatrix without missing data can be extracted from the dataset, provided by GemSeek. New couples of associations can be discovered using the same approach.

5. Final words

A typical example in the survey research is the use of ubiquitous chisquare test for association in a cross-tabulation. This test is not a tool detecting which parts of the table are responsible for this association.

Our approach is based on the association between levels of categorical variables.

Our algorithm for direct ascription of missing categorical values is based on the association between row points and column points discovered by correspondence analysis.

An open question is how to extract association between combinations of levels of categorical variables. The following features of the correspondence analysis: the percentages of inertia and squared correlations should also be involved in a machine learning algorithm.

Acknowledgements. The work of Veska Noncheva and Maria Dobreva is partially supported by the Fund NPD, Plovdiv University “Paisii Hilendarski”, under Grant SP15-FMIIT-015.

References

- [1] Dempster A. P., Laird N. M., Rubin D. B. (1997). Maximum likelihood estimation from incomplete data via the EM algorithm (with discussion). *Journal of the Royal Statistical Society, Series B*, **39**, 1–38.
- [2] Greenacre M. (2007). *Correspondence Analysis in Practice*. Second Edition. London: Chapman & Hall / CRC.
- [3] Heitjan D.F., Rubin D.B. (1991). Ignorability and coarse data. *Annals of Statistics*, **19**, 2244–2253.
- [4] Little R. J. A., Rubin D. B. (1987). *Statistical analysis with missing data*. New York: Wiley.
- [5] Murtagh F. (2005). *Correspondence Analysis and Data Coding with Java and R*, Chapman & Hall/CRC.
- [6] Nenadic O., Greenacre M. (2007). Correspondence analysis in R, with two- and three-dimensional graphics: The ca package. *Journal of Statistical Software*, **20** (3).
- [7] Rubin D. B. (1976). Inference and missing data. *Biometrika*, **63**, 581–592.
- [8] Rubin D. B. (1987). *Multiple imputation for nonresponse in surveys*. New York: Wiley.
- [9] Schafer J. L. (1997). *Analysis of incomplete multivariate data*. London: Chapman & Hall.
- [10] Schafer J. L., Graham J.W. (2002) *Psychological Methods*, Vol. 7, No. 2, 147–177

Optimal Cutting Problem

Ana Avdzhieva, Todor Balabanov, Georgi Evtimov,
Detelina Kirova, Hristo Kostadinov, Tsvetomir Tsachev,
Stela Zhelezova, Nadia Zlateva

1. Problems Setting

One of the tasks of the Construction office of company STOBET Ltd is to create large sheets of paper containing a lot of objects describing a building construction as tables, charts, drawings, etc. For this reason it is necessary to arrange the small patterns in a given long sheet of paper with a minimum wastage.

Another task of the company is to provide a way of cutting a stock material, e.g. given standard steel rods, into different number of smaller sized details in a way that minimizes the wasted material.

2. Problems Description

Task 1

A large piece of paper with width $X = 1000$ mm and length $Y = 15000$ mm is given. Over this paper many small rectangles (corresponding to tables, charts, drawings, etc.) with dimensions (a_i, b_i) , $i = 1, \dots, n$ should be arranged. The goal is to arrange the rectangles in such a way that they fill the entire width of the paper using minimal length of the sheet.

Until the study group session the company has no solution to this task.

Task 2

An unlimited stock of rods with standard section and constant length L meters is available. According to the construction chart, n_i number of details with length l_i meters each, $i = 1, \dots, m$ has to be cut from the stock rods. The purpose is to produce the desired quantities of details minimizing the wasted stock material.

The company handled the task using self developed algorithm which was slow and inefficient because it was based on exhaustive search.

3. Problems Identification

Both problems are identified as cutting-stock problems. In Operations Research, the cutting-stock problem is an optimization problem of cutting standardized pieces of stock material into pieces of specified sizes while minimizing material wasted. In terms of computational complexity, the problem is an NP-

complete problem reducible to the knapsack problem and it can be formulated as an integer linear programming (LP) problem. Task 2 is classic one dimensional (1D) cutting-stock problem while Task 1 is two dimensional (2D) cutting-stock problem which is more complex.

4. Formulation and Solution Approaches

Task 2: (1D) cutting-stock problem

The standard formulation for the (1D) cutting-stock problem (but not the only one) starts with a list of m orders, each requiring n_i pieces of length l_i , $i = 1, \dots, m$ that have to be cut from stock material (rod) of length L . We then construct a list of all possible combinations of cuts (often called “patterns”), associating with each pattern a positive integer variable x_j representing the number of stock material pieces to be slit using pattern j . The linear cutting-stock integer problem is then:

$$(1) \quad \begin{aligned} \min \quad & \sum_j w_j x_j \\ \sum_j a_{ij} x_j &= n_i, \quad \forall i = 1, \dots, m \\ x_j &\geq 0 \text{ and integer,} \end{aligned}$$

where a_{ij} is the number of times order i appears in pattern j and w_j is the cost (often the waste $w_j = L - \sum_i a_{ij} l_i$) of pattern j . In order for the elements a_{ij} , $i = 1, \dots, m$ to constitute a feasible cutting pattern, the following restriction must be satisfied

$$\begin{aligned} \sum_{i=1}^m a_{ij} l_i &\leq L, \\ a_{ij} &\geq 0 \text{ and integer.} \end{aligned}$$

Instead of problem (1) for minimizing the waste we prefer to consider the equivalent to it problem for minimizing the total number of utilized rods which is known also as bin packing problem:

$$(2) \quad \begin{aligned} \min \quad & \sum_j x_j \\ \sum_j a_{ij} x_j &= n_i, \quad \forall i = 1, \dots, m \\ x_j &\geq 0 \text{ and integer.} \end{aligned}$$

In general, the number of possible patterns grows exponentially as a function of m and it can easily run into the millions. So, it may therefore become impractical to generate and enumerate the possible cutting patterns.

An alternative approach uses column generation method. This method solves the cutting-stock problem by starting with just a few patterns. It generates additional patterns when they are needed. For the one-dimensional case, the new patterns are introduced by solving an auxiliary optimization problem called the knapsack problem, using dual variable information from the linear problem. There are well-known methods for solving the knapsack problem, such as branch and bound and dynamic programming. The column generation approach as applied to the cutting-stock problem was pioneered by Gilmore and Gomory in a series of papers published in the 1960s, see e.g. [2].

Modern algorithms can solve to optimality very large instances of the (1D) cutting-stock problem but their program implementations are in rule commercial and expensive. Some free software for finding approximate solutions are available.

Although the existing fast algorithm for finding the approximate solution is good enough, for specific purposes of the company STOBET Ltd. it was necessary to find an algorithm relevant to the data format they use which makes the usage of the available free software inadequate.

Task 1: (2D) cutting-stock problem

The formulation of a higher dimensional cutting-stock problem is exactly the same as that of the one dimensional problem given in (1) and (2). The only added complexity comes in trying to define and generate feasible cutting patterns. The simplest two dimensional case is one in which both the stock and ordered sizes are rectangular which is exactly our case.

5. Group Suggestions and Solutions

- For the 2D cutting-stock problem: we proposed a *genetic type algorithm*.
- For the 1D cutting-stock problem: we proposed a *greedy type algorithm*.

5.1. A Genetic Type Algorithm for Task 1: (2D) Cutting-Stock Problem

Genetic algorithms are a robust adaptive optimization method based on biological principles. A population of strings representing possible problem solutions is maintained. Search proceeds by recombining strings in the population. The

theoretical foundations of genetic algorithms are based on the notion that selective reproduction and recombination of binary strings changes the sampling rate of hyperplanes in the search space so as to reflect the average fitness of strings that reside in any particular hyperplane. Thus, genetic algorithms need not search along the contours of the function being optimized and tend not to become trapped in local minima [3].

According to the given objective in Task 1, near optimal solution can be absolutely acceptable. In such situations heuristics is one of the most used ways in solving optimal cutting problems. The difficulties in 2D variation of the problem come from the need that all rectangles should be properly arranged in the x axis and in the y axis simultaneously.

IDEA OF THE GENETIC ALGORITHM (GA)

The proposed GA goes in the following steps:

1. Initialization;
 WHILE (stop criteria is not met)
 BEGIN
2. Selection;
3. Crossover;
4. Mutation;
5. Evaluation;
 END
6. Report results.

When GAs (Genetic Algorithms) are applied there are three common operations to be implemented: problem data encoding, crossover, mutation and selection. In the case of 2D cutting problem we propose following parameters [1]:

- Problem data encoding is done by representing all rectangles with top/left coordinate, width, height and orientation. Rectangles are presented in stored ordered list as chromosome in the GA (known in the literature as permutation encoding);
- Single cut point crossover is implemented, applied by the rules of GA's permutation encoding;

- Mutation operator consists of random rotation of a rectangle into the resulting chromosome and random swap between two rectangles into the resulting chromosome;
- Selection operator is based on uniform random distribution, but result chromosome always replaces the worst chromosome in the population. By this selection approach elitism rule is applied indirectly.

Some modifications were done from the original form of the GAs. At first place, one part of the chromosomes are randomly shuffled, second part is descending ordered by rectangles width and third part is descending ordered by rectangles height in the initialization phase. At second place, one part of the chromosomes are filled with all rectangles in portrait orientation, second part of the chromosomes are filled with all rectangles in landscape orientation and third part of the chromosomes rectangles are in mixed orientation. All this modifications are done in order better genetic diversity to be presented during initialization part of the algorithm.

Fitness value evaluation is done by additional procedures for packing [1]. Because we do not keep information inside the chromosomes for the 2D placement of the rectangles, the additional packing procedure fill the drawing sheet of paper with proper amount of rectangles and after that the used length of paper is calculated and applied as chromosome fitness value. Packing procedure proposed in [1] is also near optimal. It does not search for the best optimal packing. Near optimal packing is fast enough and for better arrangements GA is responsible.

5.2. A Greedy Type Algorithm for Task 2: (1D) Cutting-Stock Problem

Let unlimited quantities of steel rods with different sections (types) having standard lengths L_k are given. Any such rod is said to be of type k . Let the cutting length l_c be given.

As input the details needed for the corresponding project are given. For each detail are known its label, section and length l_i . The number of items with these properties n_i that have to be cut is also known. In Table 1 is given a sample of real data provided by STOBET Ltd.

As output we need for any section (type) k of stock material the number of rods utilized for producing all items with section k , the way that any of these rods was cut (i.e. which items are cut from it and in which order) as well as the waste from any utilized rod and the total percentage of waste obtained from all utilized rods of section k .

Table 1. Sample data

label	section	number, n_i	length, (mm) l_i , mm	single weight (kg/m)	element weight (kg)	total weight (kg)
L windows 9	L 50 × 4	20	5790	3.0500	17.66	353.19
L windows 10	L 50 × 4	2	4912	3.0500	14.98	29.96
plank 20	PLATE 6 × 80	20	170		0.84	16.70
plank 33	PLATE 6 × 80	4	105		0.52	2.07
plank 36	PLATE 6 × 80	24	100		0.49	11.76
plank 47	PLATE 5 × 70	10	70		0.19	1.89
plank 48	PLATE 5 × 180	10	70		0.49	4.91
plank 49	PLATE 5 × 205	3	70		0.56	1.68
plank 50	PLATE 5 × 205	3	63		0.50	1.51
profile 25	100 × 80 × 5	19	5950	9.4900	56.47	1072.84
profile 26	SHS 100 × 4	3	5950	12.0000	71.40	214.20
profile 27	RHS 100 × 50 × 5	6	5800	10.9000	63.22	379.32
profile 28	RHS 100 × 50 × 5	6	5720	10.9000	62.35	374.09
profile 29	SHS 100 × 4	3	3020	12.0000	36.25	108.74
profile30	100 × 80 × 5	1	1000	9.4900	9.49	9.49
profile 31	SHS 100 × 4	6	780	12.0000	9.36	56.16
profile 40	EQA 70 × 7	2	70	7.3800	0.52	1.03
profile 41	EQA 70 × 7	45	55	7.3800	0.41	18.27
profile 42	SHS 100 × 4	6	3974	12.0000	47.69	286.13
profile 44	SHS 40 × 4	24	246	4.4600	1.10	26.33
profile 45	SHS 40 × 4	60	230	4.4600	1.03	61.56
profile 46	SHS 40 × 4	36	230	4.4600	1.03	36.94
profile 47	SHS 40 × 4	16	200	4.4600	0.89	16.06
profile 54	EQA 70 × 7	2	6995	7.3800	51.62	103.25
profile 55	EQA 70 × 7	2	6990	7.3800	51.59	103.17
profile 56	EQA 70 × 7	9	3880	7.3800	28.63	257.71
profile 57	EQA 70 × 7	2	3880	7.3800	28.63	57.27
profile 58	EQA 70 × 7	10	3880	7.3800	28.63	286.34
profile 59	EQA 70 × 7	1	3880	7.3800	28.63	28.63
profile 60	EQA 70 × 7	11	1675	7.3800	13.84	152.21
profile 61	EQA 70 × 7	2	1670	7.3800	13.80	27.60
profile 62	EQA 70 × 7	9	1670	7.3800	13.80	124.21

IDEA OF THE GREEDY ALGORITHM

Sort the details by their section (type).

For details with any particular section k :

- (1) Set $L = L_k$ and make an ordered list S of all items sorted in descending order by their lengths. All items i with $l_i > L$ are labeled as impossible for cutting

Table 2. Details of section EQA 70×7

	detail	n_i	l_i , mm
1	profile 40	2	70
2	profile 41	45	55
3	profile 54	2	6995
4	profile 55	2	6990
5	profile 56	9	3880
6	profile 57	2	3880
7	profile 58	10	3880
8	profile 59	1	3880
9	profile 60	11	1875
10	profile 61	2	1870
11	profile 62	9	1870

(this is caused by constructive error and the input data have to be corrected) and they are excluded from S .

(2) Take a stock rod of section k . Denote its unused part (remainder) by L_r , so $L_r = L$.

(3) If $S \neq \emptyset$, then take from S the first item i with $l_i \leq L_r$, cut it from the rod and update the remainder $L_r = L_r - l_i - l_c$ and the list $S = S \setminus \{i\}$ (i.e. discard the item i from the list).

If $S = \emptyset$ then STOP.

If $L_r < \min_{i \in S} l_i$ then the cutting of the current rod is terminated, the waste is $l_w = L_r$ and go to (2). Otherwise, go to (3).

The proposed greedy algorithm provides approximate solution.

As a rough estimate for the minimal number of rods that have to be utilized for the solution, one may take the maximum of the numbers k_1 and k_2 , where k_1 is the the smallest integer greater than or equal to the total length of all items divided by L , and k_2 is the number of items with length $l_i > L/2$.

For the sample data in Table 1 the approximate solution obtained by the proposed algorithm is presented in Table 5.

To illustrate how the greedy algorithm works on the sample data given in Table 1, we consider section EQA 70×7 which is known to be of length $L = 6000$ mm and recall the cutting length is $l_c = 5$ mm. In Table 2 there are 11 different details with this section.

The proposed greedy algorithm was implemented in JAVA, Lisp, MS Excel. Many experimental tests were made with significant amount of data provided by STOBET. The suggested greedy algorithm improved significantly the speed of finding an approximate solution. How near to the optimal solution is the

Table 3. List S of details of section EQA 70×7

detail	section	n_i	l_i , mm
profile 54	EQA 70×7	2	6995
profile 55	EQA 70×7	2	6990
profile 56, 57, 58, 59	EQA 70×7	22	3880
profile 60	EQA 70×7	11	1675
profile 61,62	EQA 70×7	11	1670
profile 40	EQA 70×7	2	70
profile 41	EQA 70×7	45	55

obtained one depends of the distribution of the particular item lengths. Because of the nature of the company projects this distribution is in most cases even. For the sample data it is shown in Figure 1.

Table 4. Solution for section EQA 70×7 with $L = 6000$ mm

number of rods	pattern	3880	1675	1670	70	55	wastage, l_w
1	t_1	1	1	0	2	4	45
5	t_2	1	1	0	0	7	15
1	t_3	1	1	0	0	6	75
4	t_4	1	1	0	0	0	435
11	t_5	1	0	1	0	0	440

For convenience, details with the same length are considered as details of one and the same type. Of course, they keep their own different labels and after the cutting is completed it is clear from which rod and at which place on it they were cut.

In this example all items with length 3880 mm are considered as one kind of detail and the same is for items with length 1670 mm. So, finally we have 7 details and 95 items, see Table 3.

If there are some $l_i > L$ the algorithm excludes them from consideration. Here this is the case for details labeled “profile 54” and “profile 55”.

So, we start with the first rod. After cutting one item of third length $l_3 = 3880$ mm, the remainder of the rod becomes $L_r = 2115$ mm. The first item in S with length $l_i \leq L_r$ is 1675 mm and we cut it from the rod. Then the remainder becomes $L_r = 435$ mm. We cut one item with $l_6 = 70$ mm and so on. At the end for the first rod we obtain remainder $L_r = 45$ mm which is smaller than the smallest item length and therefore the wastage for this rod is $l_w = 45$ mm. For the considered example the obtained cutting patterns, the number of rods used for each pattern and the waste obtained in using that pattern are given in Table 4.

Total number of the utilized for the solution rods of section EQA 70×7 is 22. In this particular case we succeed in obtaining an exact solution. Indeed, as it can be seen from the values of k_1 and k_2 for this section in Table 5 the number of utilized rods can not be smaller than 22 and for our solution we utilize exactly 22 rods. In fact, for all sections in the sample data we obtain exact solution as it can be seen from Table 5.

The approximate solution obtained by the previously used by STOBET Ltd algorithm for this sample data utilized 30 rods.

Table 5. Utilized rods for the obtained by greedy algorithm solution for data in Table 1

section	k_1	k_2	number of utilized rods	$w, \%$
L 50×4	21	22	22	4,75
PLATE 6×80	2	0	2	46.17
PLATE 5×70	1	0	1	87.50
PLATE 5×180	1	0	1	87.50
PLATE 5×205	1	0	1	92.85
$100 \times 80 \times 5$	20	20	20	48.75
SHS 100×4	10	12	12	22.88
RHS $100 \times 50 \times 5$	12	12	12	3.96
SHS 40×4	6	0	6	11.49
EQA 70×7	21	22	22	5.13

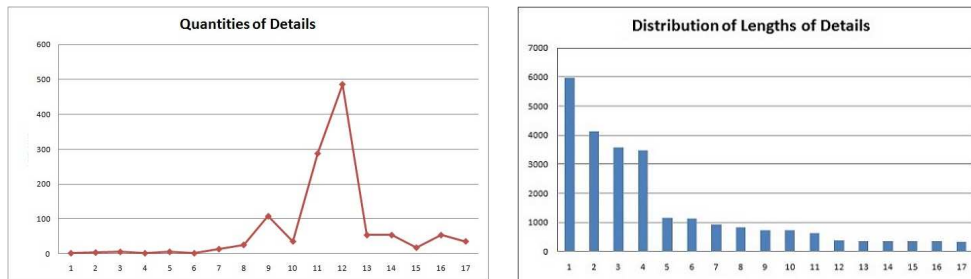


Fig. 1. Items quantities and length distribution

For solving (1D) cutting-stock problem we also applied the developed for the (2D) cutting-stock problem genetic algorithm. Doing this for the sample data the approximate solutions obtained from both algorithms (greedy and genetic) utilized the same number of rods but, of course, in some cases they differ in patterns of cuts.

Further Improvement of the Greedy Algorithm

A rod with a big remaining L_r will appear in few cases in the obtained by the greedy algorithm approximate solution in cutting rods with stock length L . If L_r of the last utilized rod is greater than $0,7L$ then it is relevant to try to permute the items in some of the patterns in order to cut the few items from the last rod from the other utilized rods.

For the obtained approximate solution, the waste from each utilized rod is known. The number and the lengths of details cut from the last rod are also known. Let their lengths be $d_1 > d_2 > d_3 > \dots$.

Create a list \bar{S} of all utilized rods (except the last one) ordered by their appearance in the solution.

Details are already sorted by length in descending order. For detail i with length l_i we seek a detail j with length $l_j > l_i$ such that the permutation of one item of length l_i and one item of length l_j between two different rods from \bar{S} is possible. Set $\varepsilon = l_j - l_i$, and call a rod from where l_i is cut rod i , and a rod from where l_j is cut rod j . Let the waste of rod i be w_i , and the waste of rod j be w_j . If we permute l_i and l_j between rod i and rod j , then w_i will become $w_i + \varepsilon$, while w_j will become $w_j - \varepsilon$. The permutation (i, j) is possible if $w_j - \varepsilon \geq 0$. A possible permutation (i, j) is useful if $w_i \geq d_k$ for some d_k because after the permutation an item of this length (or smaller) can be cut from rod i instead from the last rod. If we succeed in finding enough useful permutations, the cut of the last rod will be saved.

Preliminary part:

Find the possible permutations:

For all detail i with length l_i find the maximal waste from all rods in which cutting item with length l_i is involved and denote it as \bar{w}_i .

For any detail i with length l_i set $j = i + 1$ and create the triple $(\bar{w}_i, \bar{w}_j, l_j - l_i)$. If $\bar{w}_j \geq l_j - l_i$ the permutation (i, j) is labeled as possible and the next couple $(i, j + 1)$ is considered, if not no more j are considered for possible permutation with i .

Find the useful permutations:

For any possible permutation (i, j) the smallest k with $\bar{w}_i + l_j - l_i \geq d_k$ will be used for labeled it as k -useful. If such k does not exist the permutation is useless.

Main part:

For item with length d_1 , if there is no 1-useful permutation the algorithm stops. If not, 1-useful permutation (i, j) is done. As a result one item with length d_1 is cut from rod i . Rods i and j have to be deleted from \bar{S} . Maximal

Table 6. Initial data for RHS example
with $L = 6000$ mm and $l_c = 5$ mm

section	n_i	l_i , mm
RHS $100 \times 50 \times 4$	2	5975
RHS $100 \times 50 \times 4$	4	4135
RHS $100 \times 50 \times 4$	6	3575
RHS $100 \times 50 \times 4$	2	3473
RHS $100 \times 50 \times 4$	6	1153
RHS $100 \times 50 \times 4$	2	1127
RHS $100 \times 50 \times 4$	14	910
RHS $100 \times 50 \times 4$	26	810
RHS $100 \times 50 \times 4$	108	716
RHS $100 \times 50 \times 4$	36	715
RHS $100 \times 50 \times 4$	288	612
RHS $100 \times 50 \times 4$	486	365
RHS $100 \times 50 \times 4$	54	350
RHS $100 \times 50 \times 4$	54	340
RHS $100 \times 50 \times 4$	18	334
RHS $100 \times 50 \times 4$	54	330
RHS $100 \times 50 \times 4$	36	320

wastes \bar{w}_i and \bar{w}_j have to be recalculated if necessary and the labels of (i, j) have to be corrected if necessary. This is repeated for all items with d_1 , then for items with d_2 , etc.

At the end, either there are left some items with length d_k and no k -useful permutations are available in which case we keep the former approximate solution, or all items with lengths d_k are cut in result of permutations and the obtained in that way approximate solution is better than the former one (number of utilized rods is decreased by 1).

In place of the main part, the genetic algorithm can be used. When the initial set of useful permutations (i, j) is identified, then the index set of details I can be divided in two parts – I_1 will be the indexes of details involved in useful permutations, and I_2 will be $I \setminus I_1$.

Then the utilized rods \bar{S} can be divided into two parts: \bar{S}_1 consists of all rods from which is cut at least one detail i involved in useful permutation and $\bar{S}_2 = \bar{S} \setminus \bar{S}_1$. We need only to permute items which are in rods from \bar{S}_1 . Hence, input of the genetic algorithm will be all items cut from rods from \bar{S}_1 as well as the items cuts from the last rod. The rods from \bar{S}_2 and the rods obtained after the greedy algorithm is applied will form the new and possibly better approximate solution. If the result obtained by the genetic algorithm is not satisfactory one

Table 7. Input data for genetic algorithm used for re-optimization in RHS example

section	n_i	l_i , mm
RHS $100 \times 50 \times 4$	5	3575
RHS $100 \times 50 \times 4$	2	3473
RHS $100 \times 50 \times 4$	2	1127
RHS $100 \times 50 \times 4$	14	910
RHS $100 \times 50 \times 4$	26	810
RHS $100 \times 50 \times 4$	108	716
RHS $100 \times 50 \times 4$	36	715
RHS $100 \times 50 \times 4$	2	612
RHS $100 \times 50 \times 4$	4	365
RHS $100 \times 50 \times 4$	2	320

can enlarge the input adding in relevant way some possible permutations.

To illustrate the above, consider RHS example. Data are given in Table 6.

The greedy algorithm obtains approximate solution for which the number of utilized rods is 109, and the total waste is 18836 mm, or 2.88%. The solution is such that from the last rod only two items with length 320 mm are cut.

Permutations (1127, 910), (910, 810), (910, 716), (910, 715), (810, 716), (810, 715) are identified as useful. This means that as input for the genetic algorithm we have to consider the items cut from rods numbered from 8 to 36 in the former solution and the two items with length 320 mm. The input for the genetic algorithm for RHS example is given in Table 7. The expected result of 29 rods is achieved and the re-optimization was successful in this case. After re-optimization the number of rods utilized for the new approximate solution is 108, the total waste is 12836 mm, or 1.96%.

6. Feedback from STOBET Ltd.

The company has already successfully applied the proposed algorithms and solutions. STOBET Ltd reported:

- TASK 1: The Genetic type algorithm is very powerful. For short time we can obtain sufficiently good results. We will built-in this method in our practice.
- TASK 2: The greedy type algorithm is very fast and it is sufficiently good for many cases. Since the proposed greedy algorithm finds approximate solution it is possible in few cases to get not the most economical result,

i.e. the exact solution. Therefore we can apply proposed re-optimization or we can use memoization in dynamic optimization.

Acknowledgements. Thanks are due to Prof. Nikola Yanev for presenting to the group a thorough review of the scientific achievements in the field.

References

- [1] IICT-BAS, ESGI113, problem 3, a genetic algorithm solver,
<https://github.com/TodorBalabanov/ESGI113Problem3GeneticAlgorithmSolver>
- [2] D. Goldfarb, M. Todd. Chapter II. Linear programming, In: Handbooks in OR & MS, vol. 1 (Eds. G. L. Nemhauser et al.), Elsevier, 1989.
- [3] D. Whitley, T. Starkweather, C. Bogart, Genetic algorithms and neural networks: optimizing connections and connectivity, *Parallel Computing* Volume 14, Issue 3 (1990) 347-361.

The 2D/3D Best-Fit Problem

Velislav Bodurov, Dimo Dimov, Georgi Evtimov, Ivan Georgiev,
Stanislav Harizanov, Geno Nikolov, Vencislav Pirinski

1. Introduction and problem description

Quality control of part production is crucial in manufacturing. Whether the produced part/detail passes the inspection or not depends on its particular usage and the answer may differ from application to application. Furthermore, the daily detail manufacture is usually huge and the quality inspection should be fast. Therefore, in order to meet the needs of industry, the process must be as automatic and as flexible as possible.

Sirma Group Holding JSC is one of the largest software groups in Southeast Europe, with a proven track record since 1992. EngView Systems Jsc is a subsidiary company for CAD/CAM software, which, among other tasks, deals with quality control via scanning. More precisely, their team wants to enrich the software of the scanner they sell on the market, so that the original CAD model of the detail is “properly” compared to the scanner’s output of a given manufactured specimen. The first object usually consists of a list of “CAD primitives”, that are either line or arc segments, for which the two endpoints and the circle center/radius (for arc segments) are given. The second object is a real-point cloud, whose density depends on the scanner’s resolution. The two data sets lie in different coordinate systems, thus the scanned data should be translated and rotated in order to align with the CAD one. This “optimal” alignment is the main purpose of our work. Once achieved, the objects’ comparison is user-dependent, but typically point-wise displacements between the two data sets at certain (again user-specified) points of interest (*control points*) are measured (see Fig. 1). When those quantities are within the user-given range, the specimen passes the quality inspection.

The optimal data alignment (a.k.a. *Best-Fit problem*) can be described as a search for the best transformation matrix to transform input measured points from their coordinate system into a CAD model coordinate system using a criteria function for optimization. The best algorithmic solution should include the following features:

-
1. Partial fit (only part of the object is scanned).
 2. Different parts (these could also be measure points) can have their own

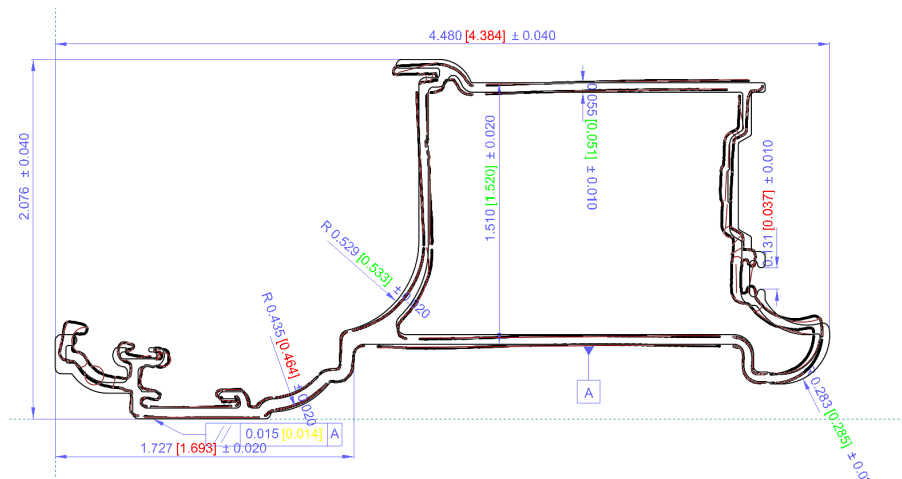


Fig. 1. CAD vs. CAM comparison of an industrial detail. Green numbers pass the quality inspection, while red ones do not

individual weights.

3. Only some of the three rotations and three translations can be applicable.
4. The algorithm can be applied on 2D or 3D data.
5. Preliminary assessment can be made if there are points that constitute noise. If such points are detected, they should be filtered out.
6. In the ideal case, the algorithm's input data – these are the data in the two coordinate systems – can appear as points, as a mesh, or as a CAD model.
7. Optimization can take place by different optimization criteria: least squares, minimum sum of deviations, mini-max, uniform deviations, minimum standard deviation, tolerance envelope, tolerance envelope mini-max.
8. The fit process should be able to accept also partially deformed parts. Even if there are discrepancies between the CAD model and the input data, the algorithm must be able to process them.
9. The computation needs to be fast and efficient.
10. An option could exist for multi-core, parallel computation.

In the discrete setting (pixel grid), a CAD/CAM Best-Fit algorithm for the corresponding raster images has been proposed and investigated in [1]. Here, because of the point-wise-distance criterion, the EngView Systems representative insisted on us working in the continuous setting (vector format), where each point is represented via its coordinates in \mathbb{R}^n , $n = 2, 3$. In [2] an algorithm that checks

if two unlabeled configurations of points in \mathbb{R}^n are an orthogonal transformation of one another is proposed. If they are, the transformation matrix is explicitly computed. This algorithm is also modified for noisy measurements (as is the case with our scanned data), but it assumes that the two point clouds are of the same cardinality and are one-to-one. The latter is not applicable to our problem, since the scanned data are randomized, thus we cannot extract their corresponding point cloud from the CAD model.

2. Our approach

The main difficulty in solving the given Best-Fit problem arises from the diversity in the data representation of the CAD model and the vectorized scanned image (*CAM data*). On the one hand, we have the CAD primitives (fully structured, continuous data), where only few points are specified (namely, the endpoints of the primitives). On the other hand, we have the real-point cloud, derived by the scanner, where the whole information is incorporated in point coordinates and no connectivity among the points is known (thus, completely unstructured, discrete data). Furthermore, the randomness of the vectorization implies that the probability for the input point cloud to contain the corresponding image of any of the CAD endpoints is zero.

Since structuring a point cloud is an NP-hard problem, we choose to discretize the CAD model and to apply techniques from Principal Component Analysis (PCA) on the two point clouds. In theory, the input data should be uniformly sampled from the specimen surface with step-size, depending on the scanner's resolution. Hence, we also uniformly sample our CAD data with respect to the arc-length parameterization of the primitives. We use a standard AutoCAD function for that. Then, for each of the discrete data sets, we compute their *energy ellipse/ellipsoid* (in 2D/3D respectively). Those ellipses define local frames, centered at the corresponding data barycenters, with axes along the directions of minimal and maximal energy. The computation is based on least-squares approach, that leads to quadratic constrained optimization problem on the unit circle. The latter is equivalent to finding the Jordan decomposition of a $n \times n$ Gramian matrix, $n = 2, 3$, which is an easy, fast, and numerically stable procedure. In signal processing, this technique is known as *the Karhunen-Loève Transform* [3] and the total mean-square error is proven to be minimized in this local (energy) basis. Finally, we map the CAM local frame onto the CAD-discretized local frame, choosing the "correct" orientation (in 2D we have 4 different options if only flips along the coordinate axes are allowed, and 8 - if we consider *mirroring*, as well) and declare the corresponding transformation matrix as optimal.

When the scanned data is denoised and uniformly sampled, while the manufactured part/detail specimen is without any defects, the transformed CAM data cloud should be perfectly contained within the continuous CAD model. Thus, the transformation matrix is optimal with respect to any optimization criteria. In practice, however, the scanned data is noisy, and the EngView Systems' team performs a denoising procedure, where untrustworthy data is erased. This, together with the possible defects of the specimen, affects the CAM local frame (mainly the coordinate axes, while the origin remains quite stable) and further "local" modifications of the derived transformation matrix are needed in order to optimize it. The latter is a subject of future work and it will be discussed in the corresponding section.

2.1. Karhunen-Loève transform

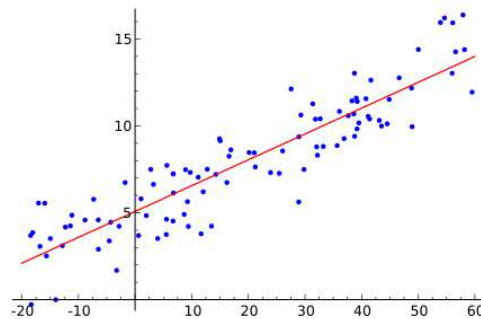


Fig. 2. Linear regression analysis. The picture is taken from Wikipedia

For a given set of N points $\mathcal{M} := \{(x_i, y_i)\}_{i=1}^N$, we look for the line in \mathbb{R}^2 that minimizes the sum of the squared Euclidean distances from the point set to it. In statistics this procedure is known as *Linear regression*, see Fig. 2 (the picture is taken from https://en.wikipedia.org/wiki/Linear_regression), while in mathematics – as *Least Squares Problem*. It is easy to show that this optimal line passes through the barycenter (x_G, y_G) of \mathcal{M} . Thus, we use the normal representation

$$\ell : A(x - x_G) + B(y - y_G) = 0$$

of the former, where $(A, B)^T$ is a unit normal vector with respect to ℓ . We want

to solve the following minimization problem

$$(1) \quad \operatorname{argmin}_{A,B} \underbrace{\sum_{i=1}^N (A(x_i - x_G) + B(y_i - y_G))^2}_{F(A,B)} \quad s.t. \quad A^2 + B^2 = 1,$$

which is equivalent to quadratic optimization on the unit circle:

$$(2) \quad \operatorname{argmin}_{A,B} \left\langle \begin{pmatrix} \langle x, x \rangle & \langle x, y \rangle \\ \langle y, x \rangle & \langle y, y \rangle \end{pmatrix} \begin{pmatrix} A \\ B \end{pmatrix}, \begin{pmatrix} A \\ B \end{pmatrix} \right\rangle \quad s.t. \quad A^2 + B^2 = 1.$$

Here, $x = (x_1 - x_G, \dots, x_N - x_G)^T$, $y = (y_1 - y_G, \dots, y_N - y_G)^T$, and $\langle \cdot, \cdot \rangle$ is the standard scalar product in \mathbb{R}^N . The matrix

$$\mathbf{M} := \begin{pmatrix} \langle x, x \rangle & \langle x, y \rangle \\ \langle y, x \rangle & \langle y, y \rangle \end{pmatrix}$$

is Gramian, thus symmetric and positive definite (unless \mathcal{M} is collinear). Problem (2) is classical. The range of the cost function F is $[\lambda_1, \lambda_2]$, where $0 \leq \lambda_1 \leq \lambda_2$ are the eigenvalues of \mathbf{M} , and the minimizer is given via

$$(3) \quad \begin{pmatrix} \bar{A} \\ \bar{B} \end{pmatrix} = \pm v_1, \quad \mathbf{M}v_1 = \lambda_1 v_1, \quad \|v_1\|_2 = 1.$$

Note that the minimizer is unique up to sign, so additional ‘‘orientation’’ issues need to be considered afterwards.

In this setup, the Karhunen-Loève transform $KL : \mathbb{R}^2 \rightarrow \mathbb{R}^2$ is simply a change of basis:

$$(4) \quad KL \begin{pmatrix} x \\ y \end{pmatrix} = \underbrace{\begin{pmatrix} v_{1,x} & v_{2,x} \\ v_{1,y} & v_{2,y} \end{pmatrix}}_{\mathcal{T}_{\mathcal{M}}} \begin{pmatrix} x + x_G \\ y + y_G \end{pmatrix}.$$

The vector v_2 is a normalized eigenvector for \mathbf{M} w.r.t. λ_2 , and it describes the direction of minimal energy of \mathcal{M} . On the other hand v_1 describes the direction of maximal energy of \mathcal{M} . In other words, the local frame (G, v_1, v_2) places \mathcal{M} along the y -axis, it is quite natural, and the most stable invariant of \mathcal{M} w.r.t. Gaussian noise.

2.2. KL-transform-based Algorithm

We propose and implement in MatLab the following algorithm in \mathbb{R}^n , $n = 2, 3$:

Algorithm 2.1 (2D/3D Karhunen-Loève transformation matrix).

Input: **cad_data**, **sc_data** *Output:* Transformation matrix \mathcal{T} and translation vector $\vec{\mathbf{d}}$

1. Compute the barycenters G^{CAD} and G^{sc} of **cad_data** and **sc_data**.
 2. Compute the shift $\vec{\mathbf{d}} = G^{CAD} - G^{sc}$.
 3. Compute \mathcal{T}_{CAD} and \mathcal{T}_{sc} as in Section 2.1.
 4. Compute the orthonormal matrix $\mathcal{T} = \mathcal{T}_{CAD}\mathcal{T}_{sc}^T$.
 5. Derive **sc_data_aligned** from **sc_data** via translation by $\vec{\mathbf{d}}$ and rotation by \mathcal{T} .
 6. **FUZZ** the **cad_data**.
 7. Axes orientation check and \mathcal{T} modifications, if necessary.
-

As already mentioned, the input **cad_data** is a point cloud, uniformly sampled from the CAD model via standard AutoCAD software. The barycenters are computed directly via coordinate-wise averaging. Since both \mathcal{T}_{CAD} and \mathcal{T}_{sc} are orthogonal, so is \mathcal{T} and it rotates the CAM local frame in order to align it with the CAD one, i.e.,

$$\mathcal{T} : v_i^{cs} \rightarrow v_i^{CAD}, \quad i = 1, \dots, n.$$

Since all the basis vectors are unique up to a sign, we have to choose the correct axes orientations for optimal data matching. The latter means that we need to consider all possible “axes flips” of the CAM data, leading to 2^n different choices, and take the one that best fits the CAD data. In 2D, those flips result in left multiplications of \mathcal{T} by

$$\mathcal{T}_x := \begin{pmatrix} 1 & 0 \\ 0 & -1 \end{pmatrix}, \quad \mathcal{T}_y := \begin{pmatrix} -1 & 0 \\ 0 & 1 \end{pmatrix}, \quad \mathcal{T}_{xy} := \begin{pmatrix} -1 & 0 \\ 0 & -1 \end{pmatrix},$$

respectively. In order to quantitatively compare the different orientations, we use another standard AutoCAD function, namely *FUZZ distance*. This works as follows: around each CAD primitive, we draw an envelope of certain width ε (the width may vary from primitive to primitive, but for the moment it suffices to consider it a global parameter) and AutoCAD orthogonally projects all points within the envelope on the primitive. (A non-scientific explanation would be, that we thicken the lines of the CAD model.) We choose an appropriate ε , and for each of the orientations of **sc_data_aligned** we count the number of points outside of the CAD model ε -envelope. The optimal orientation is the one that minimizes this number.

3. 2D Numerical examples

We consider two numerical examples (see Fig. 3). All the CAD/CAM data are provided by EngView Systems. In both cases the CAD and CAM coordinate systems are a priori aligned (Fig. 4), which does not affect at all the Karhunen-Loève Transform and the performance of Algorithm 2.1, but allows us to compare our output with the optimal transform (which is the identity). We uniformly sample the first CAD model (Fig. 3 Left) using 1323 points and the second CAD model (Fig. 3 Right) using 1218 points. The scanned data for the first example consists of 399 points, while for the second – of 8206 points. Comparison of CAD vs. CAM local bases is shown on Fig. 4. Comparisons between CAD and

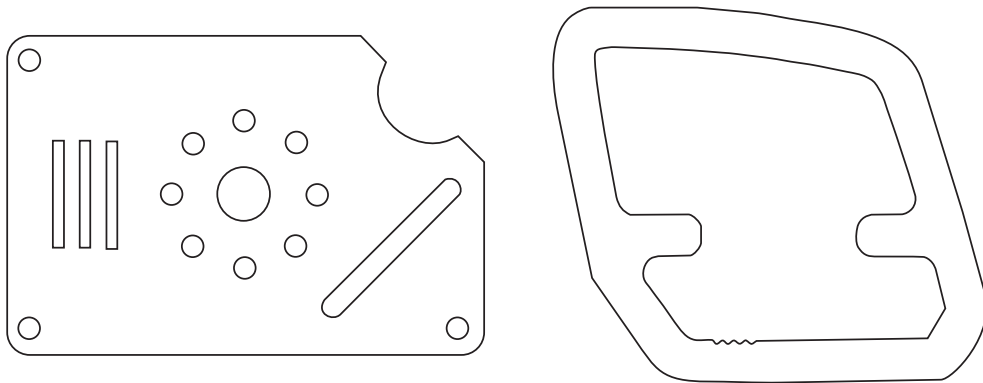


Fig. 3. The CAD models of the 2 considered parts

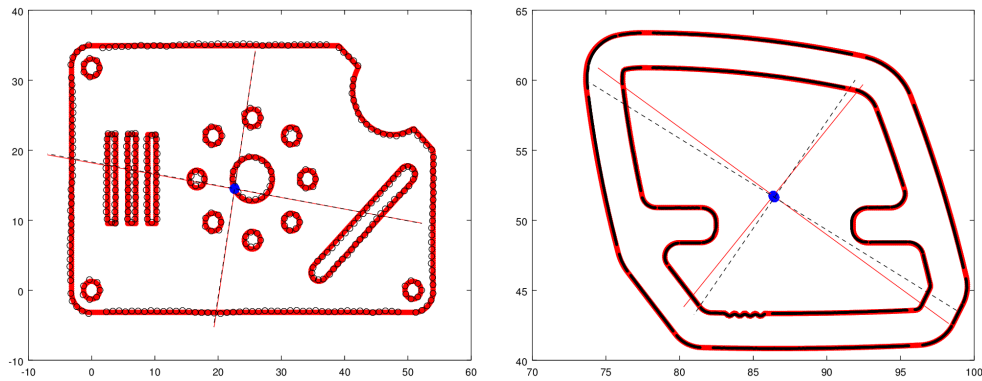


Fig. 4. Point-cloud comparison for the details: Red(solid): (Fuzzed) CAD sample and its KL frame. Black(circled): Scanned data and its KL frame. Blue dots: Barycenters

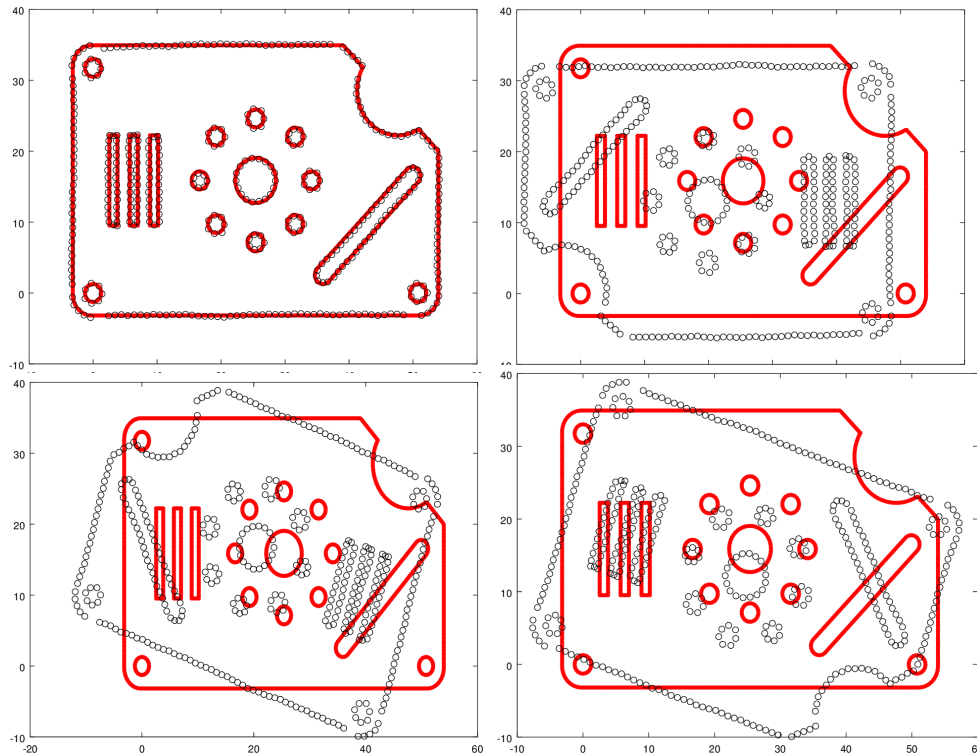


Fig. 5. Different local frame orientations for the first example

transformed CAM data w.r.t. Algorithm 2.1 are shown on top left on Fig. 5 and Fig. 6, respectively. Both scanned specimens have no manufacturing defects.

For the first example we see (almost) perfect alignment of the two KL local frames. This is due to the good specifics of both specimen and its scanning (no defects and close-to-uniform CAM sample). Moreover, even for small ε , the fuzzy CAD data incorporates almost all of the CAM points, making the orientation check in step. 7 of the algorithm straightforward (see Fig. 5).

This is not the case with the second example. There, even though the CAM sample is 20 times bigger than the one in the first example, some of the scanned data was untrustworthy and erased during the denoising process that preceded our work. This resulted into several CAD regions for which no scanning information is available (see Fig. 4). The latter polarizes the CAM point sample and affects its local axes. In turn, the outcome of Algorithm 2.1 is not the optimal transformation matrix. Furthermore, the CAD model is almost a square, thus has

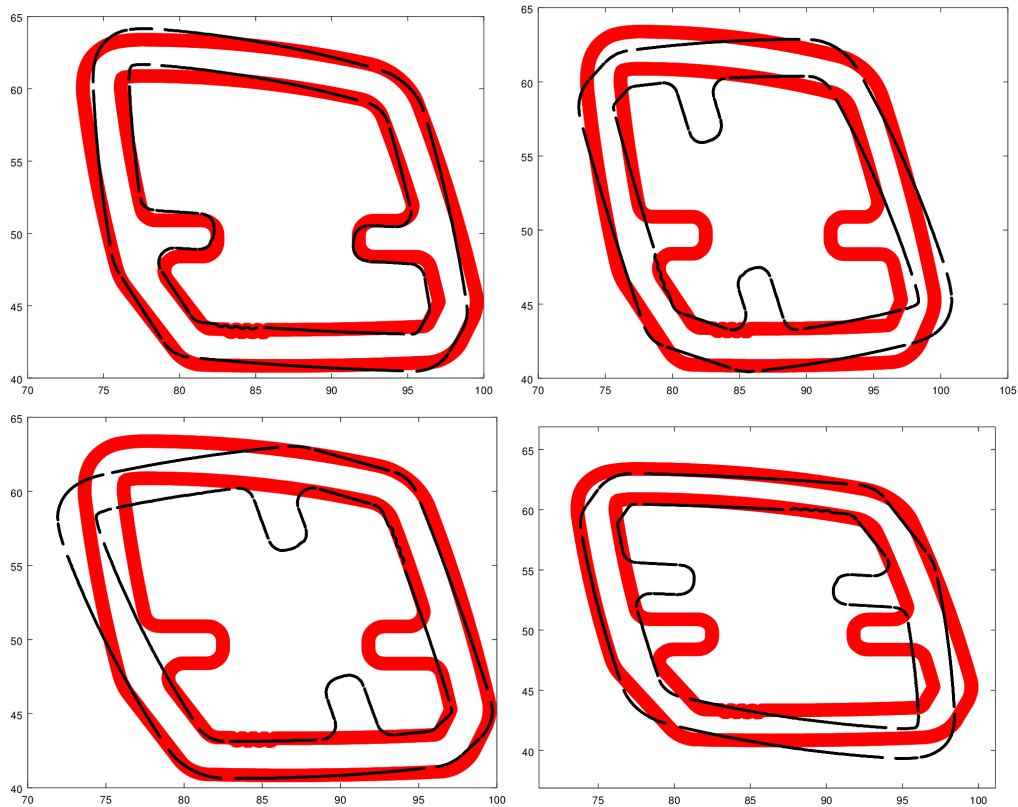


Fig. 6. Different local frame orientations for the second example

plenty of symmetries and the range of the cost function F in (1) is small. Combining the two problems, we witness a very hard orientation check (see Fig. 6). For each of the axes flips and for small ε the fuzzed CAD data contains some portions of the CAM points and misses the two “bumps”. Thus, the number of CAM points outside the fuzzed region does not differ significantly among the different orientations. In such a case, choosing the correct frame orientation is not secure, and we increase ε until a clear winner appears, namely until the “bumps” are captured by one of the candidates. The latter is indeed the correct orientation.

4. Future work

Algorithm 2.1 is just a preliminary step of the desired Best-Fit algorithm. As seen from the numerical experiments, it provides satisfactory transformation matrix only for non-deformed parts/details with uniformly sampled CAM data.

Moreover, among the desired algorithmic properties, listed in the introduction, we cover only points 4-5, because the Karhunen-Loève transform is applicable also in 3D, and Least Squares estimates are maximum-likelihood ones of Gaussian noise. Clearly, such an approach cannot deal with point 1. In order to address the remaining issues, further modifications of \mathcal{T} are necessary.

The biggest benefit of Algorithm 2.1 is that it structures $\bar{\mathcal{M}}_{sc} := \mathcal{T}(\mathbf{sc_data} + \bar{\mathbf{d}})$ in a sense that most of the scanned points away from the endpoints of CAD primitives can now be assigned to their corresponding primitive! We assume that the barycenters G^{CAD} and G^{sc} are (almost) correct. This is witnessed in both of the examples in Section 3. Moreover, Georgi Evtimov wrote a LISP function, that computes the barycenter of the continuous CAD model, and when compared to the barycenter of even random point samples (that still capture the detail geometry) we saw that the latter approximates well the former. Therefore, mainly the axes directions of the CAM local frame (but not its origin) are affected by the quality of both the detail and its scanning, so we search for another rotation matrix

$$\mathcal{R}_\theta = \begin{pmatrix} \cos \theta & \sin \theta \\ -\sin \theta & \cos \theta \end{pmatrix}, \quad \theta \in (-\pi/2, \pi/2),$$

to deal with that. Finally, the optimal rotation matrix will be

$$\mathcal{T}_{final} = R_\theta \mathcal{T},$$

while the best coordinate transform is

$$\begin{pmatrix} x \\ y \end{pmatrix} \rightarrow \mathcal{T}_{final} \begin{pmatrix} x + d_x \\ y + d_y \end{pmatrix}.$$

Let $\mathcal{M}_i \subset \bar{\mathcal{M}}_{sc}$ be the points that clearly belong to the CAD primitive P_i . Then, we can break our Best-Fit problem into N smaller and simpler ones, where N is the number of different CAD primitives in the model. Since the primitives are either line or arc segments, there are only 2 types of optimization problems that appear. Those N processes are independent and small-scale, thus they can be computed in parallel (point 10) and very efficiently (point 9). Different optimization criteria can be used (as long as the corresponding optimization problem can be numerically solved on line and arc segments!), thus point 7 is also covered. For each $i = 1, \dots, N$, given \mathcal{M}_i and (uniform sample of) P_i , the local Best-Fit problem will produce as output a rotation angle θ_i , i.e.,

$$(\mathcal{M}_i, P_i) \xrightarrow{\text{Local BestFit}} \theta_i, \quad i = 1, \dots, N.$$

The global angle θ can be a convex combination of the local ones

$$\theta = \sum_{i=1}^N \omega_i \theta_i, \quad \omega_i \geq 0, \quad \sum_{i=1}^N \omega_i = 1,$$

which addresses point 2. We can project \mathcal{T}_{final} onto any subgroup of $SO(2)$ (those, considered admissible by the user), which solves point 3.

Let us consider two different primitives P_i and P_j that are both line segments. Assuming that \mathcal{M}_i and \mathcal{M}_j are indeed scanned samples of P_i and P_j , independently of the optimization criteria the angles $\theta_i = \angle(\ell_i, P_i)$ and $\theta_j = \angle(\ell_j, P_j)$ should be equal, unless the samples are noisy or the detail is defected. Here, ℓ_i and ℓ_j are the optimal lines for \mathcal{M}_i and \mathcal{M}_j , respectively. Moreover, this equality is not affected by the accuracy of the barycenter computations, because the quantities are invariant under translation. Thus, the distribution of the set $\{\theta_i \mid P_i - \text{line segment}\}$ provides us with information about defects and/or data discrepancies (point 8).

When P_i is an arc segment, assigning the angle θ_i is not a priori clear. Furthermore, Best-Fit problems on circles are usually much more complicated than the ones on lines. For example, even the Least-Squares fit, which is a linear problem in the latter setting, has no closed form solution in the former one and there is no direct algorithm for it (see [4]). However, in our case we have additional information from the CAD model that we incorporate into the optimization problem as constraints. In particular, the center O_i and the radius R_i of the arc P_i are given, while the distance $r_i := |G^{CAD}O_i|$ can be computed. Therefore, we search for a point \bar{O}_i on the circle $C(G^{CAD}, r_i)$ for which the circle $C(\bar{O}_i, R_i)$ minimizes the least-squares functional. In other words, we restricted a 3D optimization problem (the unknowns are the coordinates of \bar{O}_i and the radius \bar{R}_i of the optimal circle) to a 1D one, where the only unknown is the angle $\theta_i = \angle \bar{O}_i G^{CAD} O_i$. The restricted problem remains nonlinear, but analyzing 1D functions is a much easier task, that, at least numerically, can be efficiently performed.

The time frame, needed for the execution of such ambitious work plan, is far beyond the one of the workshop. However, if EngView Systems are interested in further collaboration, this might be an interesting and fruitful project for both industry and science.

Acknowledgements. Geno Nikolov was partially supported by the Sofia University Research Fund through Grant 75/2015. Velislav Bodurov was partially supported by the Sofia University “St. Kliment Ohridski” under contract No. 08/26.03.2015.

References

- [1] D. Dimov, G. Gluhchev, N. Nikolov, I. Burov, E. Kalcheva, S. Bonchev, S. Milanov, B. Kiossev. The Computer System STEMB for Verification of Replicas of the Bulgarian State Emblem. *Cybernetics and Information Technologies*, 1(1):95–106, Bulgarian Academy of Sciences, Sofia, 2001.
- [2] D. Jiménez, G. Petrova. On Matching Point Configurations. In *Constructive Theory of Functions*, 141–154, Prof. Martin Drinov Academic Publishing House, Sofia, 2014.
- [3] R. D. Dony. Karhunen-Loève Transform. In *The Transform and Data Compression Handbook*, (K. R. Rao and P. C. Yip, Eds.), Boca Raton, CRC Press LLC, 2001.
- [4] N. Chernov, C. Lesort. Least Squares Fitting on Circles. *Journal of Mathematical Imaging and Vision*, 23(3):239–252, 2005.

Rigorous and Approximated Solutions of the Consolidation Problem for a Soil Layer with Finite Thickness under Cyclic Mechanical Loading

Pavel Iliev, Stanislav Stoykov, Branko Marković,
Maria Datcheva, Lyudmil Yovkov, Konstantinos Liolios,
Cihan Menseidov, Nina Müthing, Thomas Barciaga

Formulation of the problem

In poroelasticity there are two important assumptions, namely (see [2] and [6]):

- (i) the stress-strain relation for the solid matrix follows the Hooke's law for isotropic linear elastic media,
- (ii) Darcy's law governs the fluid flow within the pore system.

Using these assumptions it can be shown that the governing equation for one-dimensional (vertical) consolidation due to the time dependent mechanical loading $L(t)$, see [6], is governed by the following equation:

$$(1) \quad \frac{\partial u}{\partial t} = C_z \frac{\partial^2 u}{\partial z^2} + \eta \frac{dL}{dt},$$

where $u(z, t)$ is the excess pore water pressure at depth z and time t , C_z is the coefficient of consolidation in vertical direction z (Fig. 1) and $\eta = \frac{\alpha}{\alpha + n\beta}$. Here α , β and n are the compressibility of the solid, the compressibility of the water and the porosity, respectively. In case water is considered to be uncompressible, η equals one. The coefficient of consolidation is related to the mechanical and hydraulic characteristics of the porous medium (e.g. soil) as follows:

$$(2) \quad C_z = \frac{k K_s}{\gamma \left(1 + \frac{n\beta}{K_s}\right)},$$

where K_s is the bulk modulus of the solid phase, k is the hydraulic permeability and γ represents the fluid volumetric weight.

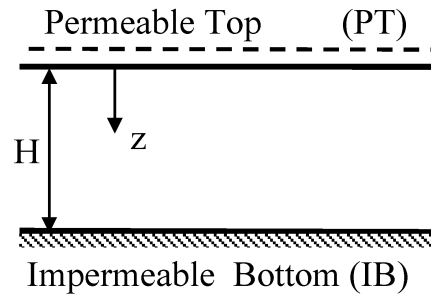


Fig. 1. Problem geometry

The boundary and the initial conditions are defined as follows (according to the notations in Fig. 1)

$$(3) \quad u(0, t) = 0, \quad \frac{\partial u}{\partial z}(H, t) = 0,$$

$$(4) \quad u(z, 0) = 0.$$

More information about the geotechnical applications and experimental data where the above formulated problem has place can be found in [5] and [4]. The task is to derive an analytical solution to the above formulated boundary value problem. Next, based on the analytical solution to evaluate the following sub-tasks:

- explicitly derive the phase shift between excess pore water pressure $u(z, t)$ and the applied load with time (for a fixed depth) especially at the bottom ($z = H, t \rightarrow \infty$), the phase shift or lag is a positive or negative delay of the excess pore water pressure as compared to the applied surface load that may vary with depth;
- parameter analysis for the solution regarding permeability k and as a function of relevant parameters (stratum depth H , bulk modulus K_s , phase shift, load amplitude q and loading period d);
- parameter analysis for the phase shift ψ as a function of the fluid and solid phase compressibility and soil permeability.

Analytical solution

In this section our task is to obtain an analytical solution for the above formulated problem. In order to do that we will first formulate the equivalent homogeneous form of Eq. (1), see e.g. [3]. For that purpose we introduce a new variable:

$$(5) \quad v(z, t) = u(z, t) - \eta \int_0^t \dot{L}(\tau) d\tau,$$

where the load function is given by

$$(6) \quad L(t) = q \sin^2 \left(\frac{\pi}{d} t \right) = \frac{q}{2} - \frac{q}{2} \cos \left(\frac{2\pi}{d} t \right).$$

Therefore Eq. (5) takes the form

$$(7) \quad v(z, t) = u(z, t) - \eta \frac{q}{2} \cos \left(\frac{2\pi}{d} t \right).$$

In the new variable v our problem is formulated as:

$$(8) \quad \frac{\partial v}{\partial t} = C_z \frac{\partial^2 v}{\partial z^2},$$

with boundary conditions:

$$(9) \quad v(0, t) = \eta \frac{q}{2} \cos \left(\frac{2\pi}{d} t \right), \quad \frac{\partial v}{\partial z}(H, t) = 0.$$

The boundary condition at the bottom of the layer ($z = H$) can be expressed as $v(H, t) = C$, where C is some constant, independent of z and t . If we assume that $C = 0$, the boundary condition at the bottom is then given as

$$(10) \quad v(H, t) = 0.$$

We seek for a harmonic solution of the homogeneous problem of the form

$$(11) \quad v(z, t) = V(z) e^{i \frac{2\pi}{d} t},$$

where the function $V(z)$ is obtained from separation of variables and thus becomes

$$(12) \quad V(z) = C_1 e^{\frac{1+i}{\sqrt{dC_z/\pi}} z} + C_2 e^{-\frac{1+i}{\sqrt{dC_z/\pi}} z}.$$

In order to obtain Eq. (12) in the form that is given, we have used the expression $\sqrt{i} = (1 + i)/\sqrt{2}$. Since the solution that we seek for is a complex function, we introduce an additional complex disturbance at $z = 0$ and hence it becomes

$$(13) \quad v(0, t) = \eta \frac{q}{2} \left[\cos \left(\frac{2\pi}{d} t \right) + i \sin \left(\frac{2\pi}{d} t \right) \right] = \eta \frac{q}{2} e^{i \frac{2\pi}{d} t}.$$

This allows us to determine the constant in Eq. (12). The solution for the variable v takes the final form:

$$(14) \quad v(z, t) = \left[C_1 e^{\frac{1+i}{\sqrt{dC_z/\pi}} z} + C_2 e^{-\frac{1+i}{\sqrt{dC_z/\pi}} z} \right] e^{i \frac{2\pi}{d} t},$$

with

$$(15) \quad C_1 = -\eta \frac{q}{2} \frac{e^{-\frac{1+i}{\sqrt{dC_z/\pi}} H}}{e^{\frac{1+i}{\sqrt{dC_z/\pi}} H} - e^{-\frac{1+i}{\sqrt{dC_z/\pi}} H}},$$

and

$$(16) \quad C_2 = \eta \frac{q}{2} + \eta \frac{q}{2} \frac{e^{-\frac{1+i}{\sqrt{dC_z/\pi}} H}}{e^{\frac{1+i}{\sqrt{dC_z/\pi}} H} - e^{-\frac{1+i}{\sqrt{dC_z/\pi}} H}}.$$

We could proceed further with obtaining the real part of the above expression, but due to the complexity of the expressed solution we follow the approach of [1]. Therefore we assume that the relation $H \gg \sqrt{dC_z/\pi}$ holds, which allows us to neglect the term with C_1 in Eq. (12) and hence

$$(17) \quad Re(v(z, t)) = \eta \frac{q}{2} e^{-\frac{z}{\sqrt{dC_z/\pi}}} \cos \left(\frac{2\pi}{d} t - \frac{z}{\sqrt{dC_z/\pi}} \right).$$

The real part in Eq. (17) is the one corresponding to the real part of the disturbance, therefore transforming the expression for the variable u yields

$$(18) \quad u(z, t) = \eta \frac{q}{2} e^{-\frac{z}{\sqrt{dC_z/\pi}}} \cos \left(\frac{2\pi}{d} t - \frac{z}{\sqrt{dC_z/\pi}} \right) + \eta \frac{q}{2} \cos \left(\frac{2\pi}{d} t \right).$$

Using this analytical solution we can have an explicit expression for the phase shift $\psi(z)$ between the excess pore water pressure and the applied load:

$$(19) \quad \psi(z) = \arctan \left[\frac{e^{-\frac{z}{\sqrt{dC_z/\pi}}} \sin \left(-\frac{z}{\sqrt{dC_z/\pi}} \right)}{1 - e^{-\frac{z}{\sqrt{dC_z/\pi}}} \cos \left(-\frac{z}{\sqrt{dC_z/\pi}} \right)} \right].$$

Thus we conclude that when $H \gg \sqrt{dC_z/\pi}$ holds the phase shift depends only on the period of the applied load and the consolidation coefficient.

Numerical solution

In this section we will find the numerical solution of our problem. The partial differential equation (1) can be written in the following form:

$$(20) \quad \frac{\partial u}{\partial t} = C_z \frac{\partial^2 u}{\partial z^2} + A \sin\left(\frac{2\pi t}{d}\right),$$

and the boundary and the initial conditions are given by Eqs. (3) and (4). The equation is discretized by the finite element method. As a result, a system of ordinary differential equations (ODE) is obtained. Because the system is linear and the time dependent mechanical loading is harmonic, the steady-state response of the system will be also harmonic. Thus, the vector of generalized coordinates is expressed by harmonic function and the system of ODE is transformed into an algebraic linear system.

Equation (1) is written in variational form, integration by parts is performed and taking into account the boundary conditions, the following equation is obtained:

$$(21) \quad \int_{\Omega} \frac{\partial u(z, t)}{\partial t} v(z) dz + C_z \int_{\Omega} \frac{\partial u(z, t)}{\partial z} \frac{\partial v(z)}{\partial z} dz = A \sin\left(\frac{2\pi t}{d}\right) \int_{\Omega} v(z) dz,$$

where $v(z)$ are the trial functions and $\Omega \in [0, H]$.

Following the standard FEM approach, the pressure $u(z, t)$ is approximated by shape functions and generalized coordinates in a local coordinate system:

$$(22) \quad u_h(\xi, t) = \sum_{i=1}^n N_i(\xi) q_i(t) \in \mathcal{V}_h,$$

where ξ is the local coordinate given by $\xi = \frac{z}{H}$ and n is the number of shape functions used in the model. In the current case, one element is used, and accuracy is achieved by adding higher order polynomials. This approach is also known as p -FEM. The shape functions $N_i(\xi)$ have to satisfy the essential boundary conditions. They are given in Figure 2. Here $q_i(t)$ are the generalized coordinates.

Switching from Ω to the reference interval $[0, 1]$ and replacing the expression for $u_h(\xi, t)$ into Eq. (21) the following system of first order ODE is obtained:

$$(23) \quad \mathbf{M}\dot{\mathbf{q}}(t) + \mathbf{K}\mathbf{q}(t) = \mathbf{F} \sin\left(\frac{2\pi t}{d}\right),$$

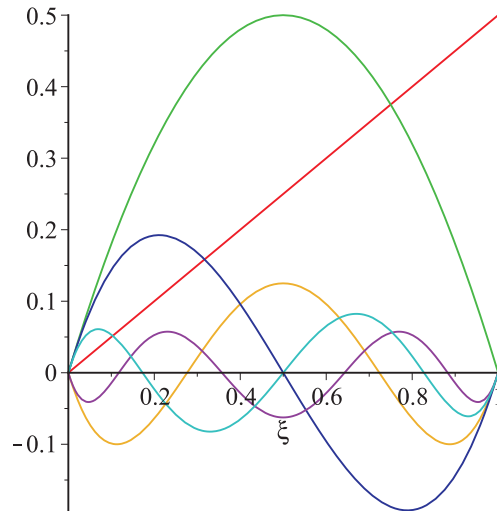


Fig. 2. Shape functions for the pressure.

where \mathbf{M} is the mass matrix, \mathbf{K} is the stiffness matrix, \mathbf{F} is the vector of generalized external forces and $\mathbf{q}(t)$ is the vector of generalized coordinates. The matrices have the following form:

$$\begin{aligned}\mathbf{M} &= H \int_0^1 \mathbf{N}(\xi) \mathbf{N}(\xi)^T d\xi, \\ \mathbf{K} &= C_z \frac{1}{H} \int_0^1 \frac{d\mathbf{N}(\xi)}{d\xi} \frac{d\mathbf{N}(\xi)^T}{d\xi} d\xi, \\ \mathbf{F} &= A H \int_0^1 \mathbf{N}(\xi) d\xi,\end{aligned}$$

where $\mathbf{N}(\xi)$ is the vector of shape functions.

Taking into account that the system is linear with harmonic excitation, the steady-state response is known to be harmonic function. Thus, the vector of generalized coordinates is expressed in the following way:

$$(24) \quad \mathbf{q}(t) = \mathbf{a} \cos\left(\frac{2\pi t}{d}\right) + \mathbf{b} \sin\left(\frac{2\pi t}{d}\right),$$

where \mathbf{a} and \mathbf{b} are vectors with the same size as \mathbf{q} . This expression for \mathbf{q} is exact for the steady-state response of the linear system. If one wants to study

the transient response of the system, a time integration method, such as Runge-Kutta should be used. Substituting (24) into the system (23), the following algebraic system is obtained:

$$(25) \quad \left(\frac{2\pi}{d} \begin{bmatrix} \mathbf{0} & \mathbf{M} \\ -\mathbf{M} & \mathbf{0} \end{bmatrix} + \begin{bmatrix} \mathbf{K} & \mathbf{0} \\ \mathbf{0} & \mathbf{K} \end{bmatrix} \right) \begin{Bmatrix} \mathbf{a} \\ \mathbf{b} \end{Bmatrix} = \begin{Bmatrix} \mathbf{0} \\ \mathbf{F} \end{Bmatrix}.$$

The vectors \mathbf{a} and \mathbf{b} are computed from this equation. These vectors determine the shape of the solution related with cos and sin terms:

$$(26) \quad u_{\cos}(\xi, t) = \sum_{i=1}^n N_i(\xi) a_i,$$

$$(27) \quad u_{\sin}(\xi, t) = \sum_{i=1}^n N_i(\xi) b_i.$$

The solution $u_h(\xi, t)$ is obtained to be (in local coordinate system):

$$(28) \quad u_h(\xi, t) = u_{\cos}(\xi, t) \cos\left(\frac{2\pi t}{d}\right) + u_{\sin}(\xi, t) \sin\left(\frac{2\pi t}{d}\right) = \sqrt{u_{\cos}(\xi, t)^2 + u_{\sin}(\xi, t)^2} \cos\left(\frac{2\pi t}{d} - \psi(\xi)\right),$$

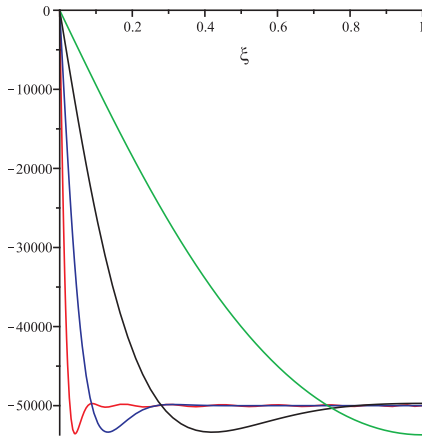


Fig. 3. $u_h(\xi, 0)$ for different values of C_z , red - $C_z = 10^{-8}$, blue - $C_z = 10^{-7}$, black - $C_z = 10^{-6}$, green - $C_z = 10^{-5}$

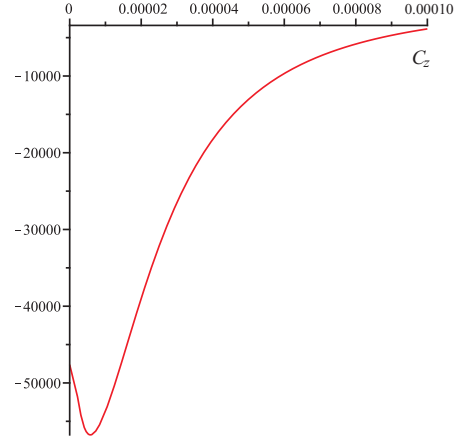


Fig. 4. $u_h(\xi, 0)$ as a function of C_z for $\xi = 1$ ($z = H$)

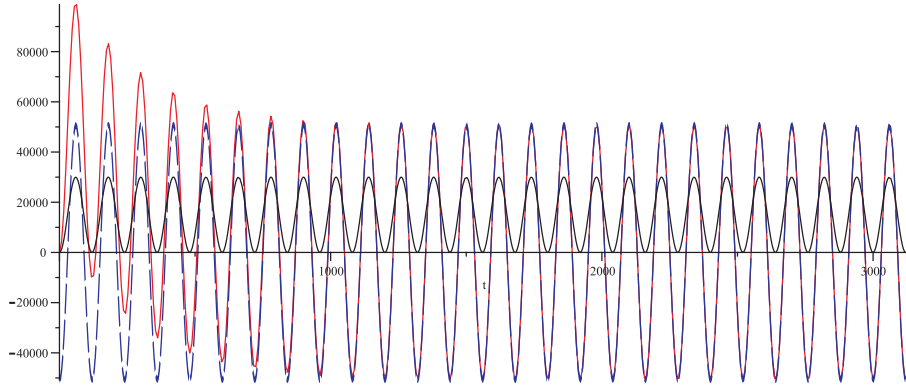


Fig. 5. $u_h(\xi, t)$ in time domain for $\xi = 1$, red – Runge-Kutta method with zero initial conditions, blue – steady-state response of the FEM, black – applied load (amplitude is increased in order to be visible in the plot)

where $\psi(\xi)$ is the phase expressed by:

$$(29) \quad \psi(\xi) = \arctan \left(\frac{u_{\sin}(\xi, t)}{u_{\cos}(\xi, t)} \right).$$

The result given for u_h in Eq. 28 is visualised in Figures 3 and 4. The comparison between the steady state and transient numerical solutions in time domain is presented in Fig. 5.

Phase shift

The explicit expression for the phase shift $\psi(z)$ as given in (19) is analyzed first. The plot for ψ as a function of the consolidation coefficient C_z is shown on Fig. 6. One can notice a drop in the phase shift when $C_z \approx 0$ and an increase after that drop. At $C_z \approx 5 \times 10^{-6}$ the slope of the graph decreases and ψ tends asymptotically to $\pi/4$.

Let us analyze in more detail the drop in the graph, i.e. negative phase shift. In Fig. 7 it is shown again a plot of ψ as a function of C_z , but now it is magnified so that one can see closely the interval with negative phase shift. From the figure we conclude that in the interval between 1.1×10^{-9} and 3.35×10^{-7} for C_z there is a negative phase shift between the excess pore water pressure and the applied load. This means that after consolidation has taken place the response from the system can be before the actual load for specific parameters. The phase shift as a function of C_z determined based on the FEM solution is given in Fig. 8.

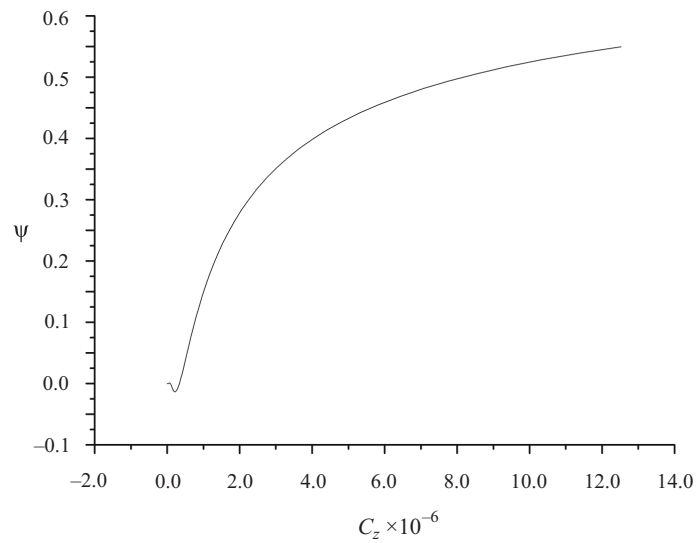


Fig. 6. Phase shift as a function of the consolidation coefficient

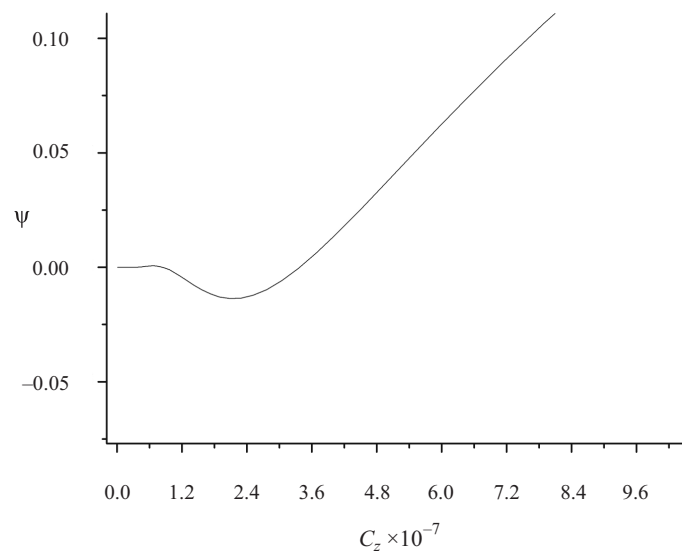


Fig. 7. Interval with negative phase shift in detail

Closing Remarks

We have shown that the analytical solution of equation (1) under reasonable assumption on the relation between frequency, permeability and layer thickness

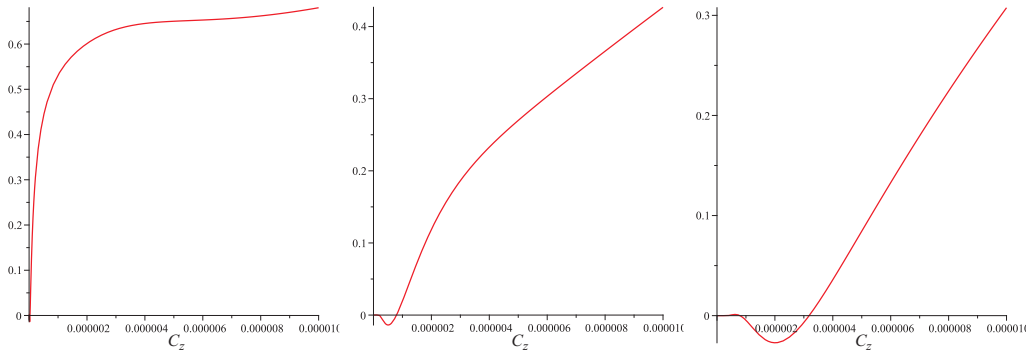


Fig. 8. Phase $\psi(\xi)$ as a function of C_z , (left) $\xi = 0.1$ ($z = 0.1H$), (middle) $\xi = 0.5$ ($z = 0.5H$), (right) $\xi = 1$ ($z = H$)

may be simplified in order to derive an analytical expression for the phase shift. Moreover, the analytical solution under this simplification is in a good agreement with the numerical solution obtained via FEM. The phase shift is presented as a function of the vertical coordinate z (depth), C_z and d by Eq. (19). On the other hand ψ may be calculated by using Eq. (29).

Acknowledgments

We would like to acknowledge the valuable help provided by Professor Nikolai Kutev from the Institute of Mathematics and Informatics at BAS.

References

- [1] F. B. J. Barends. Transient wave induced pore pressures in a stratified seabed. In *Proc. Third Conference on Scour and Erosion*, Amsterdam, The Netherlands, 2006. ICSE-3.
- [2] O. Coussy. *Poromechanics*. John Wiley & Sons, Inc., 2004.
- [3] N. Kutev, S. Tabakova and S. Radev. Approximation of the oscillatory blood flow using the Carreau viscosity model. In *2015 International Conference on Mechanics – Seventh Polyakhov’s Reading*, Saint-Petersburg, Russia, 2015.
- [4] N. Muething, T. Schanz, and M. Datcheva. On the influence of loading frequency on the pore-water dissipation during cyclic consolidation of soft soils. In Oka, Murakami, Uzuoka, and Kimoto, editors, *Computer Methods and*

Recent Advances in Geomechanics, pages 441–445, London, 2015. Taylor & Francis Group.

- [5] S. S. Razouki, P. Bonnier, M. Datcheva, and T. Schanz. Analytical solution for 1d consolidation under haversine cyclic loading. *International Journal for Numerical and Analytical Methods in Geomechanics*, 37(14):2367–2372, 2013.
- [6] A. Verruijt. *Computational Geomechanics*. Kluwer Academic Publisher, 1995.

Cyber Intelligence Decision Support in the Era of Big Data

Zlatogor Minchev, Georgi Dukov, Teodora Ivanova,
Kiril Mihaylov, Doychin Boyadzhiev, Plamen Mateev,
Maroussia Bojkova, Nina Daskalova

1. Problem Definition

Three key moments have to be solved for this complex problem proper approaching: (i) selection of suitable formalism for fast and easy modelling, implementing both experts' data and cyber incidents statistics on past and future cyberattacks trends; (ii) model quantification is necessary to be added, achieving a suitable machine interpretation for discrete optimization; (iii) some probabilistic elements have also to be considered, in order to achieve realistic models, practical implementation decision support, benefitting from the "big data" knowledge context of the task. Practical implementation of these moments will be given further.

2. Modelling & Results Optimization

The practical modelling for cyber incidents is organized in a simple and flexible manner, using the "*Entity – Relationship*" ("*E – R*") machine representation, successfully implemented in I-SCIP-SA environment [1] and being used in numerous cyber threats analysis [2].

The "*E – R*" representation is simplified in a graph-like form, noting the mathematical aspects of the current modelling efforts.

An oriented graph model of m nodes (representing the *Entities*) and n arcs (noting the *Relations* between entities in the model) is accomplished.

The arcs in the graph are marked in a quadratic $[m \times m]$ incident matrix $A = [a_{i,j}]$, $i = 1 \div m$, $j = 1 \div m$. The matrix A elements are binary numbers, regarding the presence ($a_{i,j} = 1$) or absence ($a_{i,j} = 0$) of an arc between the nodes i and j . For each arc $a_{i,j}$, a weighting coefficient $x_{i,j}$ are assumed.

The resulting classification of the graph nodes is calculated, using a cumulative approach for input $a_{k,j}$ arcs and their $x_{k,j}$ weights – p_k vs output $a_{j,k}$ arcs and their $x_{j,k}$ weights – q_k as follows:

$$(1) \quad p_k = \sum_{j=1}^m a_{kj} \cdot x_{kj}, \quad q_k = \sum_{j=1}^m a_{jk} \cdot x_{jk}, \quad k = 1 \div m.$$

In accordance with the practical necessities of cyber incidents modelling, different R^n classification zones could be defined.

An important moment here is the difficulty, related to reverse arcs' weights recalculation. A matching necessity for initial experts' nodes classification and new future beliefs trends is expected. These decision support tasks are non-trivial, producing different optimizational complexities for the multiple objects predispositioning practical needs.

A useful quadratic approach, with Euclidean L_2 norm implementation in the classification task, is proposed in [3]. As the solutions of the quadratic optimization task are not always feasible with positive arcs' weights values, a further linear simplification with D_1 as Chebyshev (cubic) norm is accomplished.

The distance D_1 of the i -th point in 2D space, following (1) the new desired predisposition (p_i, q_i) is calculated as:

$$(2) \quad D_1 = \max\left(\left|\sum_j a_{i,j} \cdot x_{i,j} - p_i\right|, \left|\sum_j a_{j,i} \cdot x_{j,i} - q_i\right|\right), \quad i = 1 \div m, \quad j = 1 \div m.$$

If we denote this D_1 distance with a new variable y , the following inequalities are obvious:

$$(3) \quad \left|\sum_j a_{i,j} \cdot x_{i,j} - p_i\right| \leq y,$$

$$(4) \quad \left|\sum_j a_{j,i} \cdot x_{j,i} - q_i\right| \leq y.$$

We use the fact that:

$$(5) \quad |x| \leq a \Leftrightarrow -a \leq x \leq a.$$

Substituting (3) and (4) modular inequalities with a couple of linear ones, following the idea in (5), we get:

$$(6) \quad -y \leq \sum_j a_{i,j} \cdot x_{i,j} - p_i \leq y,$$

$$(7) \quad -y \leq \sum_j a_{j,i} \cdot x_{j,i} - q_i \leq y.$$

Thus, introducing a new nonnegative variable y , in order to achieve minimal difference from the desired new nodes cluster positioning, we have to minimize a new linear objective function Z :

$$(8) \quad \min Z = y,$$

under linear constraints:

$$(9) \quad \sum_j a_{i,j} \cdot x_{i,j} \leq p_i + y, \quad \sum_j a_{i,j} \cdot x_{i,j} \geq p_i - y,$$

$$(10) \quad \sum_j a_{j,i} \cdot x_{j,i} \leq q_i + y, \quad \sum_j a_{j,i} \cdot x_{j,i} \geq q_i - y.$$

3. Probability Extension

The idea behind this model extension is based on the graph arcs' existence forecasting, implementing a probabilistic approach.

For each arc $a_{i,j}$ from the matrix A , the risk r for cyber attack is defined as:

$$(11) \quad r_{a_{i,j}} = h_{a_{i,j}} / u_{a_{i,j}}, \quad i = 1 \div m, \quad j = 1 \div m,$$

where h is the number of harmful requests and u – total number of requests for the $a_{i,j}$ arc.

What is also important to note here is the implemented probability distribution, benefitting from the big data knowledge context. As the combination of statistical observations, concerning past cyber incidents, have to be mixed with experts' future beliefs, a suitable approach is the Beta distribution because of its intuitive and easy implementation [4].

In this case, both the *a priori* and the *a posteriori* probabilities are defined as follows:

$$(12) \quad r_{a_{i,j}} \sim a \text{ priori } Beta(\alpha, \beta),$$

$$(13) \quad r_{a_{i,j}} \sim a \text{ posteriori } Beta((\alpha + h_{a_{i,j}}), \beta + (u_{a_{i,j}} - h_{a_{i,j}})), \quad \alpha > 0, \quad \beta > 0.$$

4. Prototyping

The studied context is outlined, following the trends noted in [5]–[10]. The “Mobile E-trading”, “Smart Mixed Realities” and “E-government Services” are selected for further exploration.

Models are created in I-SCIP-SA. The entities number is between five and seven, assuring a convenient and simple graphical illustration. 3D sensitivity diagram with four sectors (*Active*, *Passive*, *Critical* and *Buffering*) is used, following input/output (Influence/Dependence) arcs' weights cumulative assessment (see eq. (1)) with additional 3rd vector absolute sensitivity representation [1].

MS Excel 2010 SOLVER is used for the optimization support, due to the small nodes number and simplified interface [11]. The probabilistic cyber attacks simulation is organized in Matlab R2011b environment [12].

Three illustrative models (see Figure 1 – Figure 3) are developed, using STEMO Ltd. experts' support, working group discussions and research experience.

(i) Botnet DDoS attack on E-government services

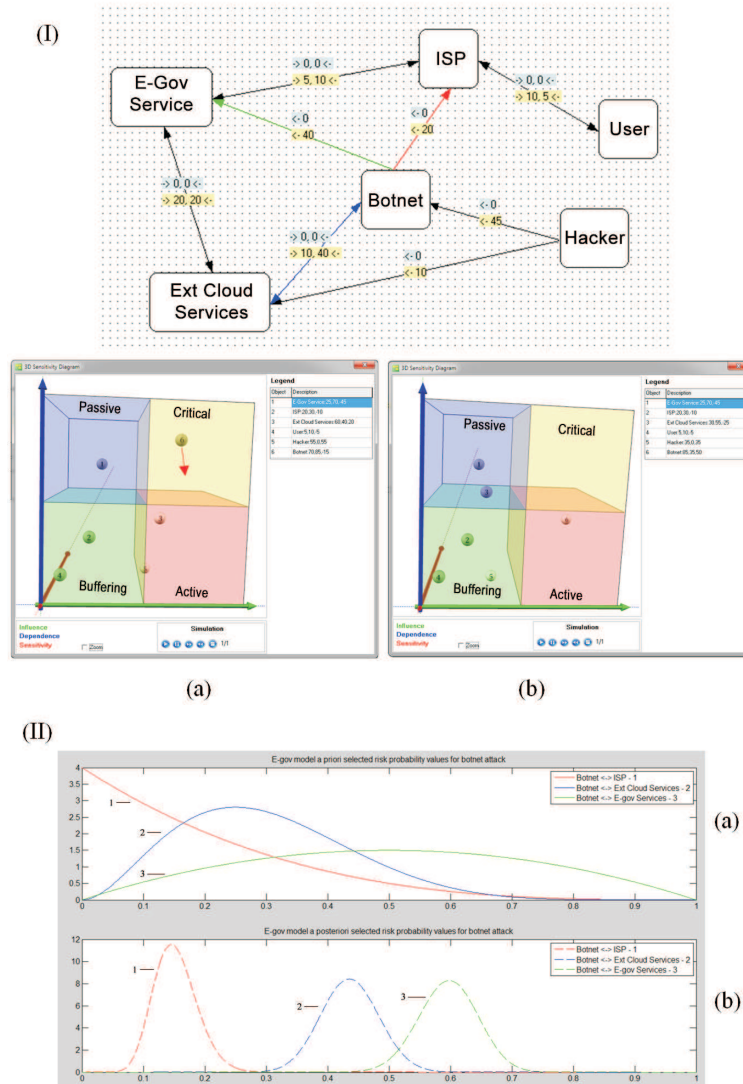


Fig. 1. E-government botnet DDoS attack system model illustration and resulting 3D sensitivity diagrams before (a) and after (b) the optimization: Panel I; Probabilistic *a priori* (a) and *a posteriori* (b) selected risk assessments: Panel II

(ii) Bank system with credit card services compromising usage via mobile devices

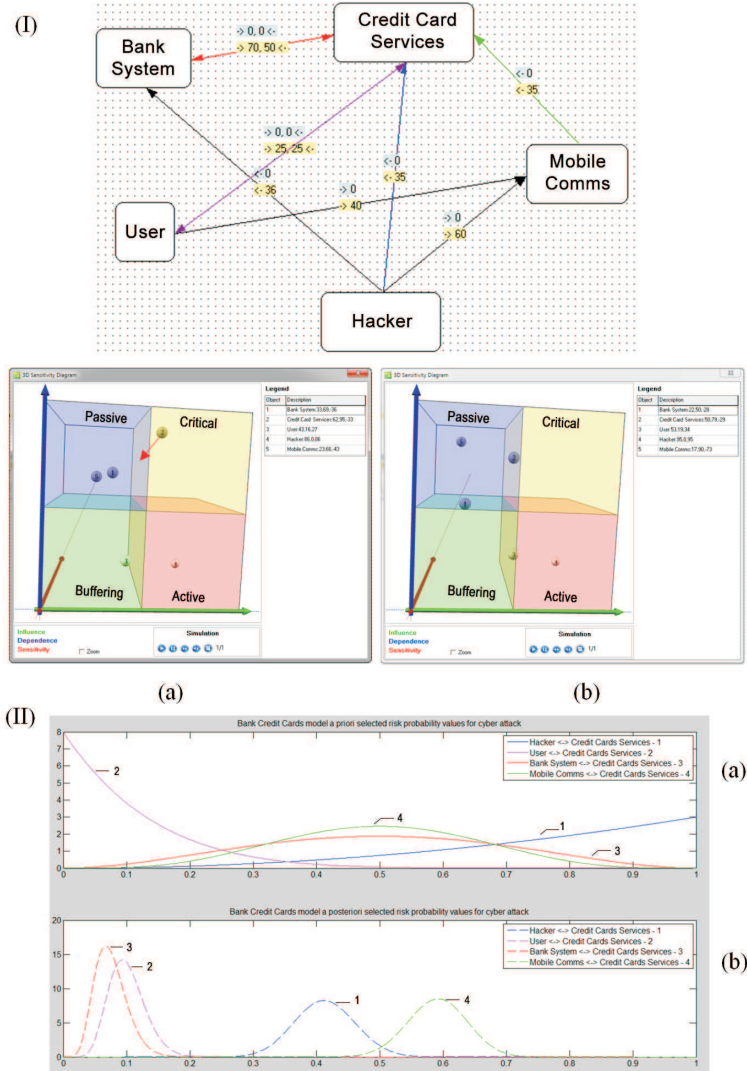


Fig. 2. Bank credit card services cyber attack system model illustration and resulting 3D sensitivity diagrams before (a) and after (b) the desired optimization: Panel I; Probabilistic *a priori* (a) and *a posteriori* (b) selected risk assessments: Panel II

(iii) Smart home mixed reality cyber attack

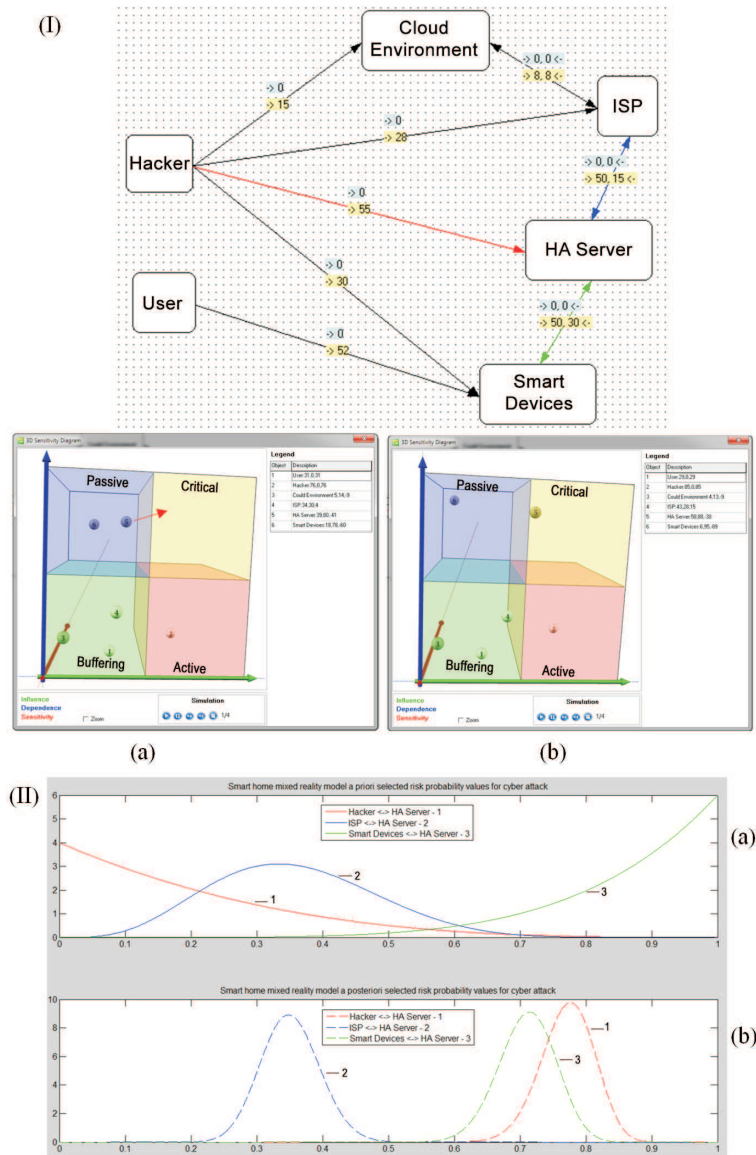


Fig. 3. Smart home mixed reality cyber attack system model illustration and resulting 3D sensitivity diagrams before (a) and after (b) the desired optimization: Panel I; Probabilistic *a priori* (a) and *a posteriori* (b) selected risk assessments: Panel II

5. Discussion

The presented complex approach for cyber intelligence decision support provides a good starting point for applied research in the era of big data.

The accomplished graph-based generic solution allows interactive analysis and near real time classification of present and future cyber threats, combining both experts' knowledge with available incidents statistics.

Additional results validation is accomplished by implementing probabilistic attacks trends evaluation, combining initial beliefs with numerical experiments simulation results.

What is also important to note here is the necessity of network sensors data integration in the presented validation approach.

This gives a possibility for deeper exploration of new cyber threats and attacks evolution, benefitting from the system modelling and assessment perspective with technologies and human factor intelligent support.

References

- [1] Zlatogor Minchev & Maria Petkova, Information Processes and Threats in Social Networks: A Case Study, In Proceedings of Conjoint Scientific Seminar Modelling and Control of Information Processes, Sofia, College of Telecommunications & Post, 2010, pp. 85–93
- [2] Zlatogor Minchev, Human Factor Role for Cyber Threats Resilience, In Handbook of Research on Civil Society and National Security in the Era of Cyber Warfare, Chapter 17, IGI Global, 2015, pp. 377–402
- [3] Zlatogor Minchev, Numerical Optimization in Support to Graph-based Scenario Modelling, In Abstracts of 13-th Workshop on Well-posedness of Optimization Problems and Related Topics, September 12–16, Borovets, Bulgaria, 2011, p. 12
- [4] Arjun Gupta & Saralees Nadarajah, Handbook of Beta Distribution and Its Applications, CRC Press, 2004
- [5] Balzarotti, D. & Markatos, E. (Eds) The Red Book – A Roadmap for Systems Security Research, SysSec Consortium, 2013, <http://red-book.eu>
- [6] Veselin Politov, Zlatogor Minchev, Pablo Crotti, Doychin Boyadzhiev, Maroussia Bojkova and Plamen Mateev, Cyber threats Optimization for E-

- Government Services, ESGI 104 Problems & Final Reports, Sofia, September 23-27, Demetra Publishing House, 2014, pp. 77–82
- [7] Threat Landscape and Good Practice Guide for Smart Home and Converged Media, Expert Report, ENISA, December, 2014, <https://goo.gl/FvuLbP>
- [8] Zlatogor Minchev, Future Threats and Challenges in Cyberspace, CSDM Views, No. 31, Centre for Security and Defence Management, Sofia, June, 2015, http://it4sec.org/bg/system/files/views_031_0.pdf
- [9] 2015 Global Megatrends in Cybersecurity, Phonemon Institute, 2015, http://www.raytheon.com/news/rtnwcm/groups/gallery/documents/content/rtn_233811.pdf
- [10] 2015 Data Breach Investigation Report, Verizon, <http://www.verizonenterprise.com/DBIR/2015/>
- [11] Christopher Zappe, Wayne Winston S. Christian Albright, Data Analysis/Optimization/Simulation Modelling with Microsoft Excel, Cengage Learning, 2011.
- [12] MoonJung Cho, Wendy Martinez, Statistics in MATLAB: A Primer, Chapman and Hall/CRC Press, 2015